THE PLANT CELL

Research Article

The NAC transcription factor FaRIF controls fruit ripening in strawberry

Carmen Martín-Pizarro [1,2] José G. Vallarino [1,2] Sonia Osorio [1,2] Victoriano Meco [1,2]
María Urrutia [1,2] Jeremy Pillet [1] Ana Casañal [1] Catharina Merchante [1] Iraida Amaya [2,3]
Lothar Willmitzer [4] Alisdair R. Fernie [4] James J. Giovannoni [5] Miguel A. Botella [1,2]
Victoriano Valpuesta [1,2,*] and David Posé [1,2,*,†]

1 Laboratorio de Bioquímica y Biotecnología Vegetal, Instituto de Hortofruticultura Subtropical y Mediterránea (IHSM), Universidad de Málaga-Consejo Superior de Investigaciones Científicas, Departamento de Biología Molecular y Bioquímica, Facultad de Ciencias, UMA, Málaga, Spain
2 Unidad Asociada de I + D + i IFAPA-CSIC Biotecnología y Mejora en Fresa, Málaga, Spain
3 Laboratorio de Genómica y Biotecnología, Centro IFAPA de Málaga, Instituto Andaluz de Investigación y Formación Agraria y Pesquera, 29140 Málaga, Spain
4 Max-Planck-Institute of Molecular Plant Physiology, Potsdam-Golm 144776, Germany
5 United States Department of Agriculture and Boyce Thompson Institute for Plant Research, Cornell University, Ithaca, NY 14853, USA

*Author for correspondence: valpuesta@uma.es, dpose@uma.es
†Senior author.

C.M.-P. generated most constructs and transgenic plants and performed and analyzed most experiments and data. J.V., S.O. and J.G performed the RNA-seq experiment of the 35Spro:RIF-RNAi lines. J.V., S.O, L.W. and A.R.F. were involved in the metabolome data acquisition and analysis. V.M., M.U., J.P. and I.A. contributed with plant in vitro maintenance and data analyses. A.C. and C.M. generated the 35Spro:RNAi binary vector and performed the transformation of those constructs. C.M.-P. M.A.B., V.V. and D.P. designed the experiments. C.M.-P., V.V. and D.P. wrote the article. All authors commented on the article.

The author responsible for distribution of materials integral to the findings presented in this article in accordance with the policy described in the Instructions for Authors (https://academic.oup.com/plcell) is: David Posé (dpose@uma.es)

Abstract

In contrast to climacteric fruits such as tomato, the knowledge on key regulatory genes controlling the ripening of strawberry, a nonclimacteric fruit, is still limited. NAC transcription factors (TFs) mediate different developmental processes in plants. Here, we identified and characterized Ripening Inducing Factor (FaRIF), a NAC TF that is highly expressed and induced in strawberry receptacles during ripening. Functional analyses based on stable transgenic lines aimed at silencing FaRIF by RNA interference, either from a constitutive promoter or the ripe receptacle-specific EXP2 promoter, as well as overexpression lines showed that FaRIF controls critical ripening-related processes such as fruit softening and pigment and sugar accumulation. Physiological, metabolome, and transcriptome analyses of receptacles of FaRIF-silenced and overexpression lines point to FaRIF as a key regulator of strawberry fruit ripening from early developmental stages, controlling abscisic acid biosynthesis and signaling, cell-wall degradation, and modification, the phenylpropanoid pathway, volatiles production, and the balance of the aerobic/anaerobic metabolism. FaRIF is therefore a target to be modified/edited to control the quality of strawberry fruits.

Open Access

IN A NUTSHELL

Background: Strawberry (*Fragaria × ananassa*) is one of the most important fruit crops worldwide, with a unique flavor and aroma and a high nutritional value that are acquired as the fruits ripen. During ripening, fruits soften and increase their levels of sugars, vitamins, the compounds responsible for the aroma, and anthocyanins, the pigments responsible for their red color. Different plant hormones participate in the regulation of strawberry fruit ripening, abscisic acid (ABA) being the major promoting ripening factor. Besides phytohormones, a few transcription regulators (transcription factors) are also known to be involved in specific aspects of strawberry fruit ripening. However, transcription factors with broader and more general roles over the course of ripening are still unknown.

Question: We identified a transcription factor, named FaRIF, whose levels dramatically increase during strawberry ripening, being therefore an excellent candidate to play an important role controlling this process. To study the role of FaRIF in the regulation of strawberry fruit ripening, we generated transgenic lines silenced for *FaRIF* by RNA interference or with increased expression, either constitutively or specifically in the strawberry fruit. We used fruits from these lines to study in detail the effects of altering *FaRIF* expression on different ripening parameters.

Findings: Our results showed that FaRIF is essential to positively regulate ripening of strawberries, controlling different key processes such as cell wall degradation, and therefore fruit softening, as well as the biosynthesis of anthocyanins, sugars, and volatiles. We also established that FaRIF controls the expression of genes involved in the biosynthesis and signaling of different phytohormones, including ABA, and that FaRIF regulates basic aspects of energy metabolism such as the aerobic/anaerobic metabolic balance, which is known to play an important role in the onset of strawberry fruit ripening. Therefore, FaRIF is an excellent biotechnological target for future modification in order to control the quality and shelf life of strawberries.

Next steps: We next wish to study the mechanisms by which FaRIF regulates strawberry fruit ripening through the identification of protein partners and the genes whose expression is directly controlled by this transcription factor.

INTRODUCTION

Strawberry (*Fragaria × ananassa* Duch.) is one of the most popular fruit crops thanks to the unique flavor and aroma of its berries, two critical quality parameters that are acquired during the ripening process. The strawberry fruit is an achenetum, consisting of a fleshy part (receptacle) that results from the development of the flower receptacle, in which the actual fruits (achenes) are embedded (Liu et al., 2020). Strawberry ripening is a genetically programmed and highly coordinated process that leads to structural and biochemical changes such as receptacle softening and increase in the contents of sugars, anthocyanins, volatile compounds, and vitamins. Strawberry fruit has been considered as a genuine example of nonclimacteric fruit ripening, which, in contrast to that of climacteric fruits, does not require ethylene to initiate and/or maintain the ripening program (Symons et al., 2012). Nevertheless, several reports have found that the application of ethylene to strawberry fruits and the generation of plants with reduced ethylene sensitivity have an effect on strawberry ripening (Trainotti et al., 2005; Villareal et al., 2010; Sun et al., 2013; Merchante et al., 2013). The main phytohormones controlling the enlargement of the strawberry fruit receptacle at early stages are auxin and gibberellic acid (GA) (Nitsch, 1950; Csukasi et al., 2011; Kang et al., 2013; Estrada-Johnson et al., 2017; Liao et al., 2018), whereas abscisic acid (ABA) is considered the main phytohormone controlling the ripening process (Jia et al., 2011). Besides ABA, other phytohormones have been proposed to be involved in specific molecular processes associated with ripening in receptacles and/or achenes such as ethylene (Merchante et al., 2013),

jasmonate (Concha et al., 2013), brassinosteroids (Chai et al., 2012), and polyamines (Guo et al., 2018).

Besides the role of different phytohormones in the control of ripening, a number of TFs have also been identified as important regulators. Among them, several TFs belonging to the MYB family have been identified and shown to be involved in regulating flavonoid accumulation such as the positive regulator MYB10 (Lin-Wang et al., 2010; Medina-Puche et al., 2013; Castillejo et al., 2020), and the repressor MYB1 (Aharoni et al., 2001), and in the biosynthesis of flavonoids and ABA (GA-induced MYB; GAMYB) (Vallarino et al., 2015), sucrose (GAMYB and MYB44.2) (Wei et al., 2018), and the volatile compound eugenol (EMISSION OF BENZENOIDS II; EOBII, which acts together with the DOF-like TF FaDOF2) (Medina-Puche et al., 2015; Molina-Hidalgo et al., 2017). In addition, other TFs have been proposed to play a role in fruit setting and ripening, such as the basic Helix–Loop–Helix (bHLH) SPATULA (FaSPT) (Tisza et al., 2010), the atypical HLH PACLOBUTRAZOL RESISTANCE1 (FaPRE1) (Medina-Puche et al., 2019), the MADS-box SHATTERPROOF-like (FaSHP) (Daminato et al., 2013), and the SEPALLATA1/2-like (FaMADS9) (Seymour et al., 2011; Vallarino et al., 2019). However, a general regulator of strawberry ripening process has not been described so far.

NAC (NAM, ATAF, and CUC) TFs constitute a large protein family that plays important regulatory roles in plant development and environmental responses (Olsen et al., 2005). These TFs are characterized by a conserved region known as the NAC domain, located at their N terminus and involved in DNA recognition, dimerization, and binding, whereas their

C terminus is highly diverse and determines the different NAC subgroups (Ooka et al., 2003). Members of this family are involved in the regulation of ripening-associated processes in fruits such as citrus (de Oliveira et al., 2011), banana (*Musa acuminata*) (Shan et al., 2012), tomato (*Solanum lycopersicum*) (Zhu et al., 2014; Kou et al., 2016), peach (*Prunus persica*) (Zhou et al., 2015), kiwifruit (*Actinidia deliciosa*) (Nieuwenhuizen et al., 2015), and apple (*Malus domestica*) (Yeats et al., 2019; Zhang et al., 2020). Recently, a total of 112 *NAC* genes were described in *F. vesca*, six of them with a potential role in the ripening process (Moyano et al., 2018). A genome-wide expression analysis of wild strawberry (*F. vesca*) *NAC* genes during abiotic and biotic stress has also been recently performed (Zhang et al., 2018). Moreover, the response to phytohormone treatments of some *NAC*s has also been tested (Moyano et al., 2018; Carrasco-Orellana et al., 2018). Among them, the expression of *FcNAC1* and the ortholog of *F. vesca* and *F. × ananassa NAC022* in beach strawberry (*F. chiloensis*) responded to ABA and auxin. FcNAC1 also activated the expression of a cell-wall remodeling enzyme, pectate lyase (*FcPL*) in vitro (Carrasco-Orellana et al., 2018). Despite all these data, there is no functional study for any NAC TF involved in strawberry fruit ripening to date.

In this study, we functionally characterized *FaNAC035*, which we renamed *FaRIF* (Ripening Inducing Factor). *FaRIF* encodes an NAC TF with the highest expression throughout strawberry fruit ripening (Sánchez-Sevilla et al., 2017). Stable transgenic lines overexpressing and silencing *FaRIF* under a constitutive promoter (cauliflower Mosaic Virus 35S) and stable lines silencing *FaRIF* from a fruit receptacle-specific promoter (*EXPANSIN2*) were established and phenotypically characterized, resulting in a clear alteration of different ripening-related parameters. Comprehensive metabolome and transcriptome analyses of the receptacle of $35S_{pro}$:*RIF*-RNAi fruits point to FaRIF as a central regulator of strawberry fruit ripening, controlling main ripening processes, such as the phenylpropanoid pathway, cell-wall structure, phytohormone metabolism, and the aerobic/anaerobic balance of the central carbon metabolism.

RESULTS

Identification of NAC TFs potentially regulating strawberry fruit ripening

To identify candidate NAC TFs playing a role in the regulation of *F. × ananassa* fruit ripening, we analyzed the expression of the 112 genes annotated as encoding NAC TFs in *F. vesca* (Moyano et al., 2018) using available transcriptome data from receptacles and achenes at four ripening stages (green, white, turning, and red), leaves and roots from *F. × ananassa* cv. Camarosa (Sánchez-Sevilla et al., 2017). Ten *NAC* genes showed increasing expression during ripening: *FaNAC006*, *FaNAC010*, *FaNAC015*, *FaNAC021*, *FaNAC022*, *FaNAC033*, *FaNAC034*, *FaNAC035*, *FaNAC042*, and *FaNAC096*, suggesting a putative role of their encoded TFs in the regulation of this process (Figure 1). Strikingly,

FaNAC035 was by far the *NAC* gene with the highest transcript levels among all ripening-induced *NAC* genes in *F. × ananassa* fruits (Figure 1A). Although the expression of *FaNAC035* in achenes was already rather high, it was even higher in receptacles (Figure 1B). We validated the expression pattern of *FaNAC035* by real-time quantitative PCR (RT-qPCR) analysis at three stages of ripening of receptacles, i.e., green, white, and red, and in two vegetative tissues, leaves, and roots (Figure 1C). Next, we generated specific antibodies against FaNAC035 and analyzed the amount of FaNAC035 protein by immunoblot analysis in receptacles during ripening (Figure 1D). Our results showed that FaNAC035 is present in receptacles at the green stage and that its level greatly increases during ripening (Figure 1D).

We next performed a phylogenetic analysis of FaNAC035 using the 112 NAC proteins from *F. vesca* (Moyano et al., 2018) as well as additional NACs belonging to different subgroups based on their C-terminal domain (Supplemental Figure S1 and Supplemental Data Set S1). Interestingly, FaNAC035 formed a monophyletic group with NACs involved in senescence, such as the NAM-B1 from peach (Guo and Gan, 2006) and the Arabidopsis NAC-REGULATED SEED MORPHOLOGY1 (NARS1) and NARS2 (Kunieda et al., 2008). FaNAC035 was also related to tomato NON-RIPENING (SlNOR), a TF-regulating climacteric ripening (Giovannoni, 2004; Wang et al., 2019), although the closest homolog to this tomato TF was FvNAC021.

Together, these data suggested that *FaNAC035* might play an important role in the regulation of strawberry fruit ripening. Thus, we selected *FaNAC035* for further characterization and named it as *FaRIF* (Ripening Inducing Factor).

FaRIF promotes strawberry fruit ripening

We cloned the *FaRIF* cDNA from ripe *F. × ananassa* cv. Camarosa fruits. The predicted FaRIF protein differed in 22 out of 343 amino acids when compared with its *F. vesca* ortholog (*FvNAC035*; FvH4_3g20700) (Supplemental Data S1 and Figure S2). In order to investigate the role of *FaRIF*, we selected a specific 265-bp sequence downstream of the conserved NAC domain coding sequence and generated a construct for gene silencing by RNA interference (RNAi) (Supplemental Data S1 and Figure S2) driven by the constitutive 35S CaMV promoter (*35Spro*:*RIF*-RNAi). We transferred four independent lines with similar fruit phenotypes to the greenhouse (Supplemental Figure S3). We selected two lines, *35Spro*:*RIF*-RNAi #3 and #11, as representative lines based on their low levels of *FaRIF* mRNA (Figure 2A). Further analysis of FaRIF protein levels in red receptacles by immunoblot analysis detected no protein accumulation in any of the $35S_{pro}$:*RIF*-RNAi lines (Figure 2B), indicating that *FaRIF* RNAi-mediated silencing was highly efficient.

Constitutive silencing of *FaRIF* did not result in altered vegetative growth or development (Supplemental Figure S4). However, visual analysis of ripe receptacles of *35Spro*:*RIF*-RNAi lines showed a lighter red color compared with control fruits at the same developmental stage (Figure 2D). We quantified color differences using the CIELAB color
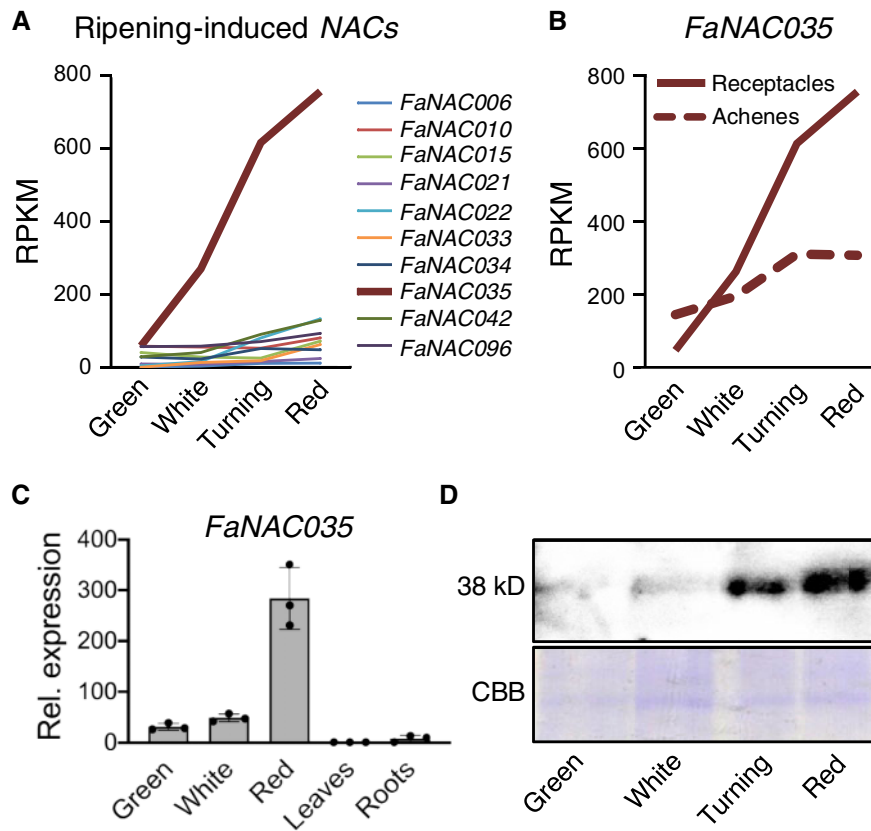
Figure 1 *FaNAC035* gene expression and protein levels dramatically increase during strawberry receptacle ripening. A, B, Expression pattern of ripening-induced NAC transcription factor genes at four ripening stages in receptacles (A), and of *FaNAC035* in receptacles and achenes (B); data from Sánchez-Sevilla et al. (2017). C, Relative expression of *FaNAC035* in wild-type fruit receptacles at three ripening stages, leaves and roots, as determined by RT-qPCR. Data are means ± se of three biological replicates. D, Immunoblot analysis in wild-type fruit receptacles at four ripening stages to detect FaRIF protein (38 kD) using anti-FaRIF antibody (upper). CBB staining of total nuclear protein extracts are shown in the bottom panel as loading control.

space values: a* (green-red spectrum), b* (blue-yellow spectrum), and L* (brightness-darkness). We observed significant differences between control and transgenic lines for L* and b*, but not for a*, indicating that silencing of *FaRIF* generates paler fruits whose color profile is enriched in the yellow part of the spectrum (Figure 2C). In addition to the receptacles, ripe achenes from the $35S_{pro}$:*RIF*-RNAi lines were also lighter in color than those in the control, indicating a role of *FaRIF* in achene ripening.

Next, we compared fruits of $35S_{pro}$:*RIF*-RNAi and control lines from green with overripe stages. For this purpose, we monitored fruits marked at the early green stage over time (Figure 2E) and calculated the percentages of fruits at different developmental stages (Figure 2F). We noticed a delay in color in $35S_{pro}$:*RIF*-RNAi fruits compared with the control after 10 days of development. Moreover, this delay in ripening progression in the RNAi lines was maintained after 30 days. At this stage, 100% of the control fruits were clearly wilted and senescent, with some showing symptoms of infection by powdery mildew. In contrast, most of the silenced fruits were hydrated and appeared healthy at the red stage (Figure 2E). Thus, the fruit phenotypes and the delayed

ripening of the RNAi lines indicated an important role of FaRIF in promoting ripening of strawberry fruits.

FaRIF controls cell-wall metabolism and fruit firmness

To identify genes associated with *FaRIF* function in fruit ripening, we performed a transcriptome deep sequencing (RNA-seq) analysis using receptacles from control and $35S_{pro}$:*RIF*-RNAi #3 and #11 lines at the white stage and at their maximum stage of ripening (hereafter called red stage). We mapped RNA-seq reads to the v4.0.a1 assembly and annotation of the *F. vesca* reference genome (Edger et al., 2018). A principal component analysis showed that PC1 separated the samples based on the developmental stages, whereas PC2 clustered the samples according to their genotypes, as $35S_{pro}$:*RIF*-RNAi #3 and #11 lines shared a similar transcriptome that was quite distinct from the control (Supplemental Figure S5A).

We calculated normalized read counts (reads per kilobase of transcript per million, RPKM) for each gene and removed genes with RPKM values lower than 1 in all the samples. With this threshold, 15,790 genes were deemed expressed
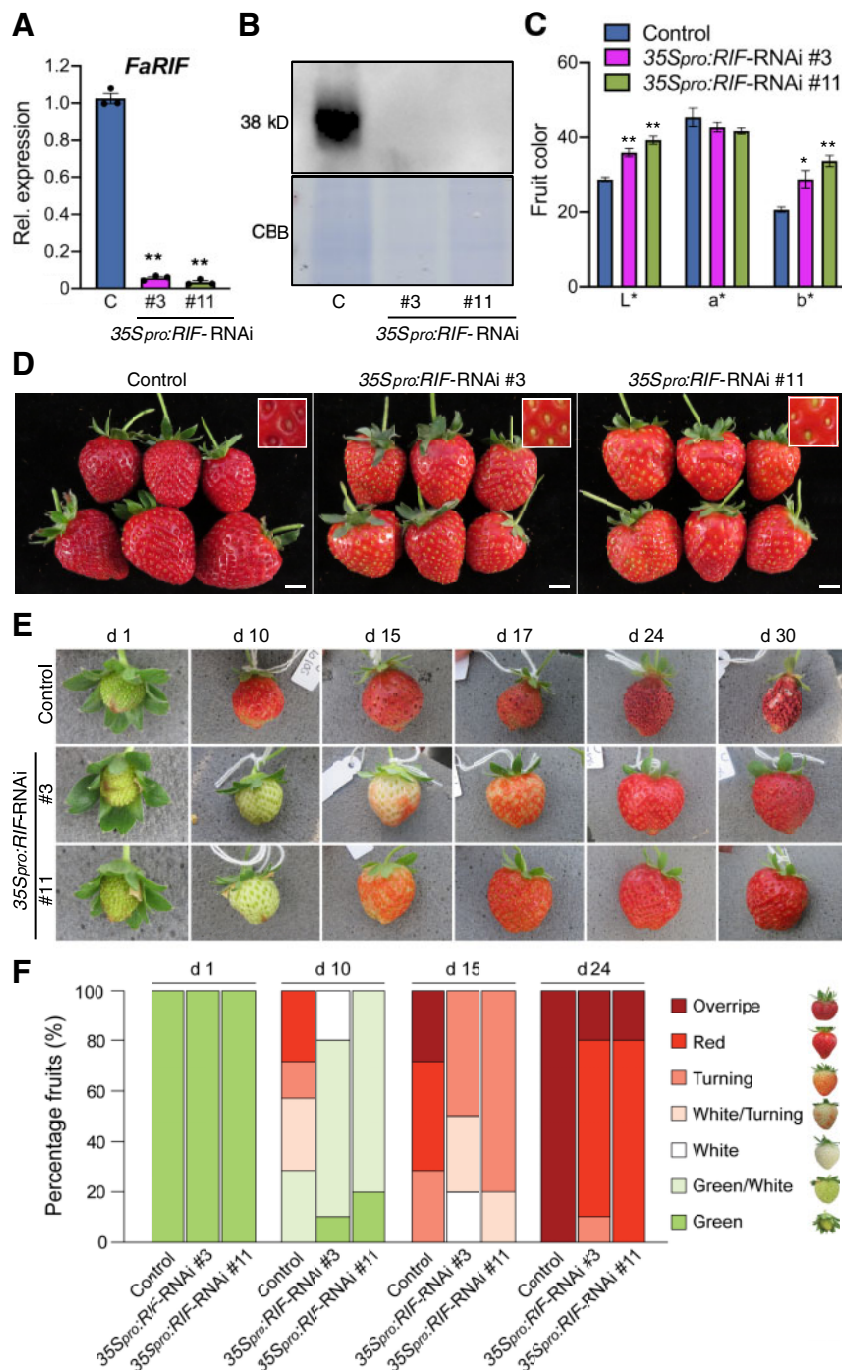
Figure 2 *35Spro:RIF*-RNAi lines show a strong silencing of *FaRIF* and display a paler red color and a delay in ripening progression. A, Relative expression of *FaRIF* in ripe receptacles from control (C) and stable *35Spro:RIF*-RNAi plants, as determined by RT-qPCR. B, Immunoblot analysis in ripe receptacles of control and stable *35Spro:RIF*-RNAi plants to detect FaRIF protein (38 kD) using anti-FaRIF antibody (upper). CBB staining of total nuclear protein extracts are shown in the bottom panel as loading control. C, Color characterization in the CIELAB color space for the lightness-darkness coefficient (L*), green-red (a*), and yellow-blue spectrum (b*). D, Fruit phenotype at the red stage in control and stable *35Spro:RIF*-RNAi transgenic lines. Inset: detail of the achenes. Scale bars, 1 cm. E, Representative pictures of a single fruit for each line at different times. A total of 10 fruits were marked at the same early green stage (Day 1), and the phenotypes were monitored 10, 15, 17, 24, and 30 days afterward. F, Percentage of fruits at each developmental/ripening stage for each time point. Ten fruits were analyzed per genotype. Data in (A) and (C) are means ± SE of 3 and 10 biological replicates, respectively, analyzed by Student's *t*-test (*P < 0.01; **P < 0.001).

from a total of 28,588 annotated genes (Supplemental Data Set S1). To determine differentially expressed genes (DEGs) between the control and both RNAi lines, we selected only genes with a false discovery rate *P*-value correction ⩽ 0.05 for each line and stage separately (Supplemental Figure 5B). We retained 1,368 DEGs at the white stage and 1,535 DEGs

at the red stage, of which 367 were differentially expressed in both lines at the two ripening stages (Supplemental Figure S5B, Data Set S2).

The transcriptome analysis confirmed that the transcript levels of *FaRIF* (*FaNAC035*) were dramatically reduced in both transgenic lines, i.e. approximately 10- and ~12-fold reduction in lines #3 and #11, respectively, at the white stage, and ~28- and ~25-fold for lines #3 and #11, respectively, at the red stage (Figure 3A; Supplemental Data Set S3), indicating that the silencing
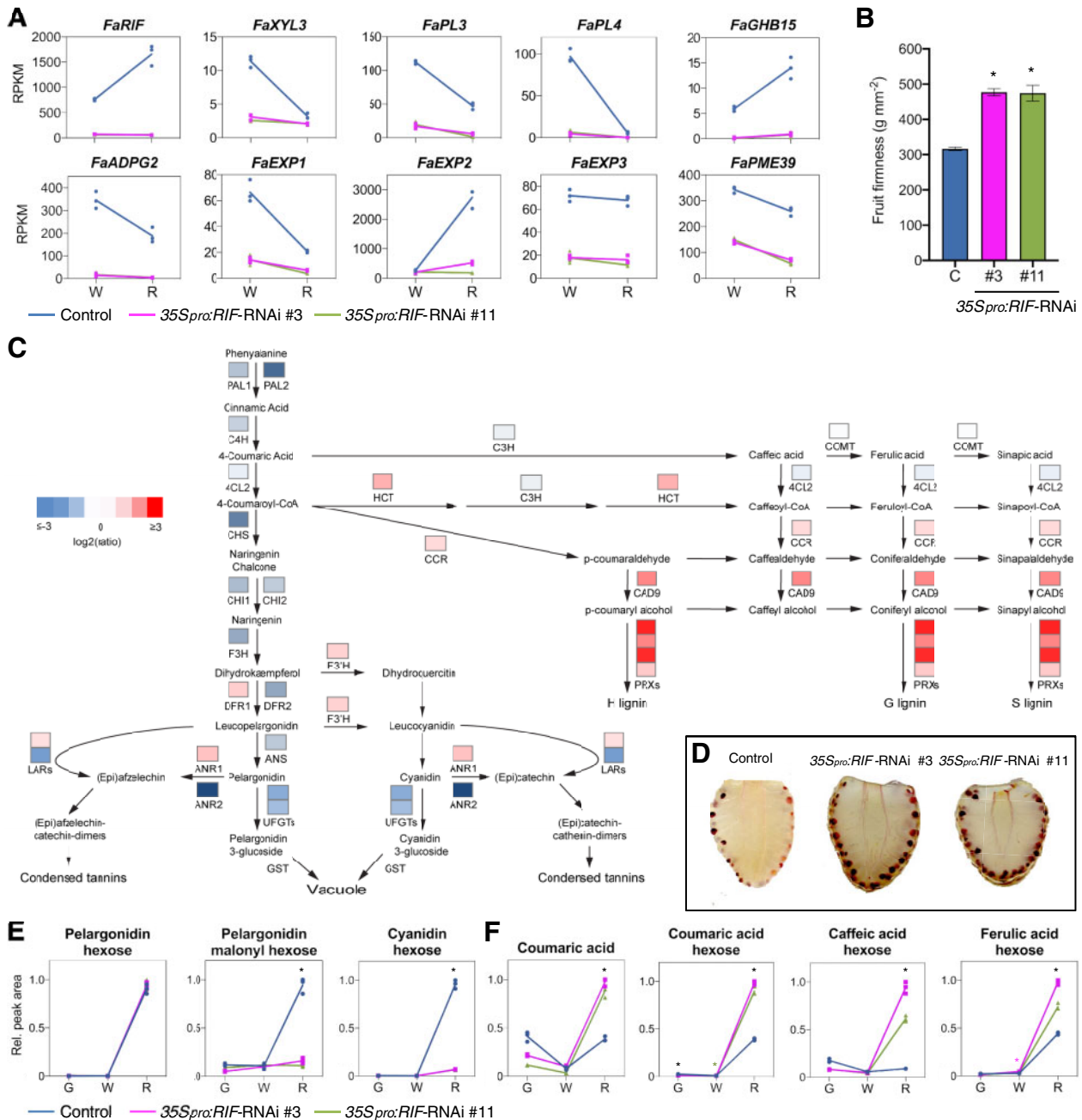
Figure 3 FaRIF controls the expression of genes involved in cell-wall degradation and the phenylpropanoid pathway, controlling fruit firmness, and anthocyanin and lignin levels. A, Expression of *FaRIF* and genes involved in cell-wall degradation and modification in control and *35Spro:RIF*-RNAi white (W) and red (R) receptacles. B, Fruit firmness measurement in control (C) and *35Spro:RIF*-RNAi ripe receptacles. Data are means ± SE of 10 biological replicates analyzed by Student's *t*-test (*$P < 0.001$). C, Phenylpropanoid, flavonoid, and lignin biosynthetic pathways. Colors denote the average of the log$_2$ of the *35Spro:RIF*-RNAi/control expression ratio in both transgenic lines at the red stage for the respective genes. Red and blue show up- and downregulation, respectively, in both silenced lines. D, Lignin staining in ripe fruit sections from control and *35Spro:RIF*-RNAi plants using phloroglucinol. Photographs were taken at the same distance. E, F, Changes in relative contents of anthocyanins (E) and hydroxycinnamic acid derivatives (F) in green (G), white (W), and red (R) receptacles of control and *35Spro:RIF*-RNAi receptacles. Data in (E) and (F) were analyzed by Student's *t* test (*$P < 0.0005$). Black asterisks indicate $P < 0.0005$ for both RNAi lines compared with the control. Colored asterisks denote $P < 0.0005$ for one of the RNAi lines compared with the control.

mediated by the RNAi construct under the *35S* promoter is very efficient. In addition to *FaRIF*, 5 out of the 10 ripening-related *NAC* genes were differentially expressed in at least one ripening stage but only *FaNAC042* was strongly downregulated in both RNAi lines at the two ripening stages (Supplemental Data Set S3). To evaluate the possibility of a possible nonspecific silencing of *FaNAC042*, we analyzed the similarity between the *FaRIF* RNAi hairpin sequence and the three *FaNAC042* homeolog sequences in *F. × ananassa*. As shown in Supplemental Figure S6, the hairpin sequence is rather different than the sequences of *FaNAC042*, suggesting that *FaNAC042* expression is regulated either directly or indirectly by FaRIF instead of an unspecific silencing. Besides these *NAC* genes, other ripening-related TF genes, as the R2R3 MYB TF *FaEOBII*, the DOF-like *FaDOF2*, and two bHLHs, i.e. *FaSPT* and *FaPRE1*, were also downregulated in the $35S_{pro}$:*RIF*-RNAi lines (Supplemental Data Set S1).

Next, we used MapMan bins (Usadel et al., 2009) in order to identify categories of genes or pathways enriched among the DEGs identified with a more than two-fold up- or downregulation in the RNAi lines (Supplemental Data Set S4). The decrease in strawberry fruit firmness during ripening is due to the activity of cell-wall degradation and remodeling enzymes (Posé et al., 2011). Fittingly, at the white stage, "cell wall" was one of the most enriched MapMan category, with several subcategories significantly enriched as well (Supplemental Figure S7 and Data Set S4). Thirteen out of the 16 genes of the "cell-wall degradation" subcategory were downregulated in $35S_{pro}$:*RIF*-RNAi white receptacles, including genes encoding for a β-xylosidase (*FaXYL3*), two pectate lyases (*FaPL3* and *FaPL4*), an endo-1,4-beta-glucanase (*FaGH9B15*), and a polygalacturonase (*ARABIDOPSIS DEHISCENCE ZONE POLYGALACTURONASE* 2; *FaADPG2*), three of which (*FaPL3*, *FaGH9B15*, and *FaADPG2*) being also downregulated at the red stage (Figure 3A). Genes related to cell-wall modification were also downregulated in the RNAi lines, such as expansins (*FaEXP1*, *FaEXP2*, and *FaEXP3*), a pectin methylesterase (*FaPME39*), and arabino galactan-proteins (*FaAGPs*) (Dotto et al., 2006; Xue et al., 2020; Pérez-Pérez et al., 2018) (Figure 3A). Interestingly, other genes associated with cell-wall disassembly were upregulated in the RNAi lines such as pectate lyase 2 (*FaPL2/plB*), polygalacturonase 1 (*FaPG1*), *FaPME38*, and rhamno-galacturonate lyase 1 (*FaRGlyase1*) (Jiménez-Bermúdez et al., 2002; Benítez-Burraco et al., 2003; Quesada et al., 2009; Xue et al., 2020; Molina-Hidalgo et al., 2013) (Supplemental Figure S8A). These data support a significant modification of the cell-wall composition and assembly in *FaRIF*-RNAi fruits. Consistent with the altered expression of these cell-wall-related genes and the delayed ripening phenotype, the receptacles of the $35S_{pro}$:*RIF*-RNAi lines were significantly firmer than those of the control (Figure 3B).

FaRIF regulates the phenylpropanoid pathway, the accumulation of anthocyanins and lignin, and the expression of aroma-related genes

Changes in the content of phenolic compounds have been widely reported during strawberry fruit ripening, including anthocyanins, which are responsible for the red color of mature receptacles and achenes (Fait et al., 2008; Härtl et al., 2017). In agreement, MapMan analysis showed that the "secondary metabolism" bin was significantly enriched during the red stage, including numerous genes involved in the phenylpropanoid pathway (Supplemental Figure S7B and Data Set S4). Indeed, key genes in the initial steps of the pathway were significantly downregulated in red fruits of $35S_{pro}$:*RIF*-RNAi plants, including the phenylalanine ammonia lyases genes *PAL1* and *PAL2*, cinnamic acid 4-hydroxylase (*C4H*), and 4-coumaroyl-CoA ligase (*4CL2*) (Figure 3C). Interestingly, the branching point leading to either the flavonoid or monolignol pathways showed a differential pattern. *CHS1*, encoding chalcone synthase 1, which is responsible for the first committed step in the flavonoid pathway, and most of the downstream genes were downregulated. Conversely, genes of the monolignol pathway, such as those encoding for hydroxycinnamoyltransferase, the cinnamoyl-CoA reductase, and the cinnamyl alcohol dehydrogenase 9, were upregulated (Figure 3C), suggesting an enhanced activity of this branch of the pathway.

In order to analyze to what extent these transcriptome changes might affect the profile of secondary metabolites, we performed a metabolome analysis using ultra performance liquid chromatography coupled to tandem mass spectrometry, extending the analysis to green, white, and red developmental stages (Supplemental Figure S9, Data Set S5). We detected significant changes in some anthocyanins and phenolic acids and their derivatives at the red stage (Figure 3, E and F; Supplemental Figure S9A). In particular, we observed a drastic reduction for cyanidin hexose, one of the major anthocyanidins responsible of the reddish-purple color and the minor pelargonidin malonyl hexose in the transgenic lines in comparison to the control (Figure 3E). However, we saw no differences for pelargonidin hexose or pelargonidin rutinose, responsible for the orange color. These changes may thus explain the lighter color and the enrichment in the yellow part of the color spectrum observed in ripe *FaRIF*-silenced fruits (Figure 2, C and D). Consistent with the transcriptome data, red receptacles of the RNAi lines showed an increase in the precursors of lignin biosynthesis, such as coumaric acid and the hexose derivatives of the coumaric, caffeic, and ferulic acids (Figure 3F). To determine whether the different hydroxycinnamic acid levels resulted in differences in lignin content, we performed histochemical staining of red fruits of control and $35S_{pro}$:*RIF*-RNAi lines. As shown in Figure 3D, receptacles of the $35S_{pro}$:*RIF*-RNAi lines showed increased staining relative to control lines in the vasculature and achenes, indicating a higher lignification in ripe *RIF*-silenced fruits.

Volatiles play an important role in the aroma of strawberry fruits. The accumulation of these compounds is closely related to changes in secondary metabolism during fruit ripening. To test whether FaRIF plays any role in the regulation of volatile production, we analyzed the expression in the receptacles of 35S$_{pro}$:RIF-RNAi lines of a number of genes reported to be involved in volatile biosynthesis in strawberry. Interestingly, the expression of *FaEOBII* and *FaDOF2*, which act synergistically to activate the transcription of *EUGENOL SYNTHASE2* (*FaEGS2*) and positively regulate the biosynthesis of the phenylpropanoid eugenol (Molina-Hidalgo et al., 2017), was downregulated in red fruits from the 35S$_{pro}$:RIF-RNAi lines (Supplemental Figure S8B). Furthermore, the expression of *FaEGS2* was also downregulated in ripe *FaRIF*-silenced fruits (Supplemental Figure S8B). Moreover, the red receptacles of 35S$_{pro}$:RIF-RNAi lines also showed a lower expression of *NEROLIDOL SYNTHASE1* (*FaNES1*) (Supplemental Figure S8B), involved in the biosynthesis of the terpenic volatile compounds linalool and nerolidol (Aharoni et al., 2004). These results suggest that FaRIF might be important to control the biosynthesis of compounds responsible for strawberry fruit aroma during the ripening process.

FaRIF regulates phytohormone cross-talk to control ripening

Strawberry fruit development and ripening are coordinated by a tightly controlled phytohormonal cross-talk (Liao et al., 2018; Gu et al., 2019). Our transcriptome analysis showed that the "Hormone metabolism" MapMan bin was also significantly enriched among DEGs between 35S$_{pro}$:RIF-RNAi and control receptacles at both ripening stages (Supplemental Figure S7 and Data Set S4). This category included genes related to the metabolism and signaling of ABA, the main phytohormone controlling strawberry fruit ripening as well as auxin, ethylene, and polyamines (Supplemental Table S1). Interestingly, the gene encoding the rate-limiting enzyme in ABA biosynthesis, 9-cis-epoxycarotenoid dioxygenase (*FaNCED3*), was significantly downregulated in *FaRIF*-silenced fruits at both ripening stages (Figure 4). Furthermore, the most expressed *NCED* in strawberry receptacles, *FaNCED5* (Liao et al., 2018), also named *FaNCED2* (Gu et al., 2019), was also downregulated in red receptacles of the silenced lines, although it was only significant in line #11 (Supplemental Data Set S3). Moreover, the ABA biosynthetic encoding gene encoding zeaxanthin epoxidase (*FaZEP*) was downregulated at the red stage (Figure 4A). In addition, a number of genes involved in ABA signaling were also differentially expressed, including *FaHVA22*, the protein kinase-encoding gene *SUCROSE NONFERMENTING1-RELATED PROTEIN KINASE 2.6* (*FaSnRK2.6*), and two TF-encoding genes, the light-responsive TFs *ELONGATED HYPOCOTYL5* (*FaHY5*) and the B-box-containing protein 19 (*FaBBX19*) (Shen et al., 2001; Han et al., 2015; Chen et al., 2008; Bai et al., 2019) (Figure 4A; Supplemental Table S1).

The down- or upregulation in the expression of all these genes would support a lower ABA content in 35S$_{pro}$:RIF-RNAi receptacles, which in turn might result in altered ripening progress in these lines. To investigate this possibility, we quantified the concentration of ABA in ripe receptacles, revealing a significant reduction in ABA content of 16%–25% in 35S$_{pro}$:RIF-RNAi red receptacles compared with that of control fruits (Figure 4B). This result supports our hypothesis that *FaRIF* acts upstream of ABA to regulate strawberry fruit ripening. Infiltration of ABA in strawberry receptacles induces ripening, as reflected by color formation (Moyano-Cañete et al., 2013; Li et al., 2016). We thus infiltrated green receptacles of 35S$_{pro}$:RIF-RNAi lines with 100 µM ABA and mock solutions. Interestingly, receptacles infiltrated with ABA developed color faster than mock-infiltrated fruits (Figure 4C), supporting a role for *FaRIF* in controlling ripening-associated changes such as the biosynthesis of anthocyanins through the regulation of ABA biosynthesis.

In addition to ABA, other phytohormones play an important role in strawberry fruit development and ripening (Liao et al., 2018; Gu et al., 2019). Our transcriptome analysis identified a number of genes involved in auxin biosynthesis or signaling that were differentially expressed in both white and red 35S$_{pro}$:RIF-RNAi receptacles, such as the cytochrome P450 gene *CYP79B*, the TF-encoding gene *AINTEGUMENTA-LIKE6* (*AIL6*), or the auxin repressor gene *Aux/IAA 9* (*IAA9*) (Sugawara et al., 2009; Krizek et al., 2016; Ulmasov et al., 1997) (Supplemental Table S1). Supporting an altered ABA and auxin content in the RNAi receptacles, the transcript levels of three ABA- and auxin-responsive TF genes, i.e., *FaSHP*, *ABA-STRESS-RIPENING* (*FaASR*), and *FaNAC022*, the ortholog to *FcNAC1* (Daminato et al., 2013; Jia et al., 2016; Carrasco-Orellana et al., 2018), were also altered at both white and red stages (Supplemental Table S1). Furthermore, genes involved in the ethylene signaling pathway were upregulated, whereas genes involved in polyamines biosynthesis were downregulated in 35S$_{pro}$:RIF-RNAi white and red receptacles (Supplemental Table S1). These data support an important role for FaRIF in controlling the phytohormonal balance during strawberry fruit ripening not only by inducing ABA biosynthesis but also potentially by regulating the biosynthesis and signaling of other strawberry development and ripening-related phytohormones such as auxin, ethylene, and polyamines.

FaRIF regulates primary metabolism inhibiting glycolysis and fermentation

Carbohydrate metabolism is another key process controlling fruit growth and development (Kanayama, 2017). A good example is sucrose, which, in addition to being a major determinant of fruit quality, functions as a signal promoting ABA accumulation and strawberry fruit ripening (Jia et al., 2013). Therefore, we analyzed primary metabolites in receptacles of control and 35S$_{pro}$:RIF-RNAi transgenic lines at the green, white, and red developmental stages by gas chromatography-mass spectrometry (GC–MS). Most of the metabolites
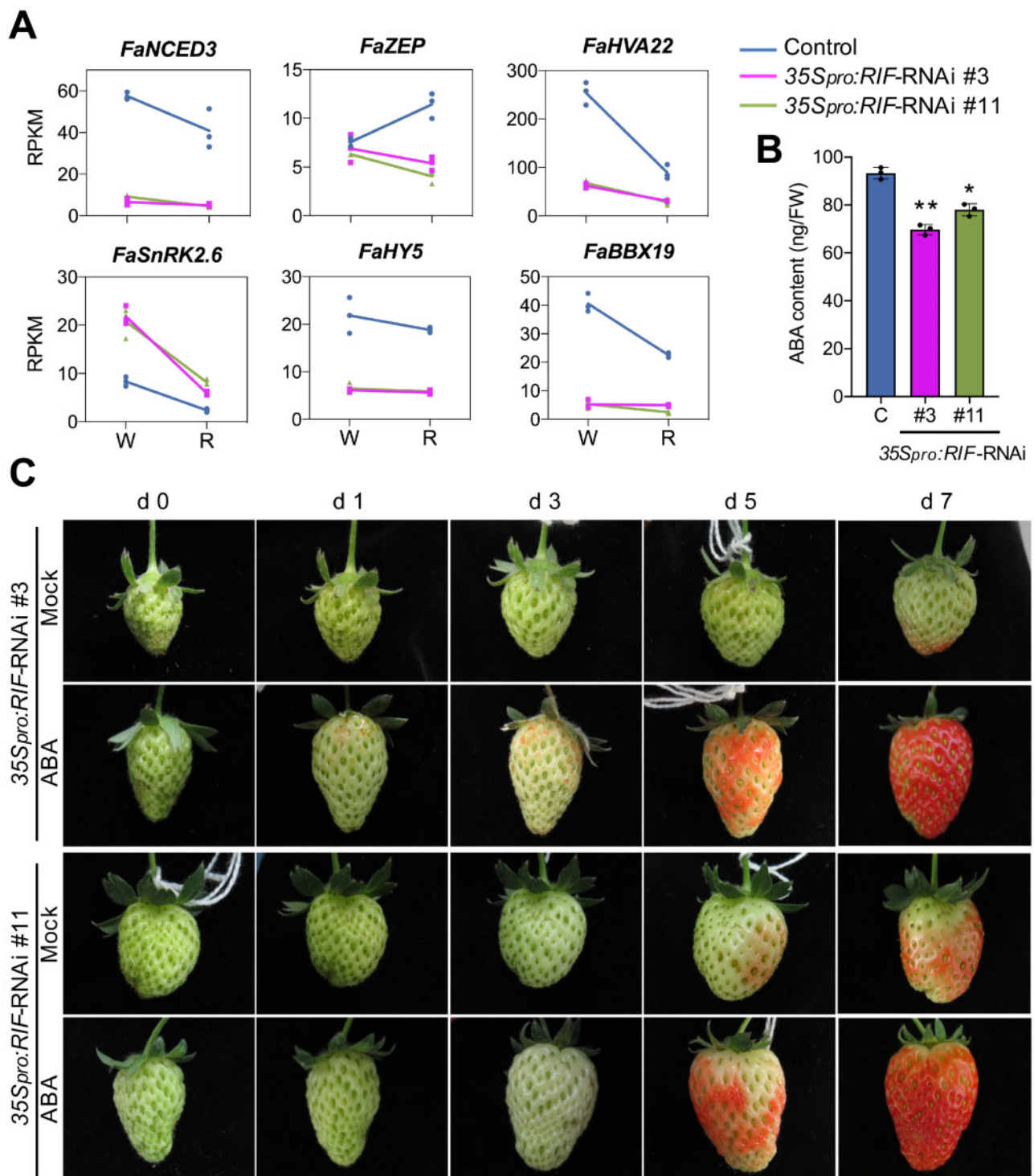
Figure 4 FaRIF regulates ABA biosynthesis and response. A, Expression of ABA biosynthetic (*FaNCED3* and *FaZEP*) and -responsive (*FaHVA22* and *FaSnRK2.6*) genes in control and *35Spro:RIF*-RNAi white (W) and red (R) receptacles. B, ABA content (ng/FW) in control (C) and *35Spro:RIF*-RNAi red receptacles. Data are means ± SE of three biological replicates, analyzed by Student's *t* test (*$P < 0.005$; **$P < 0.0005$). C, Ripening progression in *35Spro:RIF*-RNAi receptacles 7 days after mock-infiltration with 2% ethanol or 100 μM ABA. Representative pictures of a single fruit for each *35Spro:RIF*-RNAi line in each condition out of three biological replicates are shown. Fruit size cannot be directly compared across panels.

analyzed showed differences in silenced fruits from both transgenic lines compared with the control, at least at one stage (Supplemental Figure S9B and Data Set S6). Remarkably, main sugar levels were altered in the RNAi lines.

Indeed, although glucose and fructose levels significantly increased in red *35Spro:RIF*-RNAi receptacles, their sucrose content was significantly reduced (Figure 5A). These changes in main sugars were reflected in a lower content of soluble
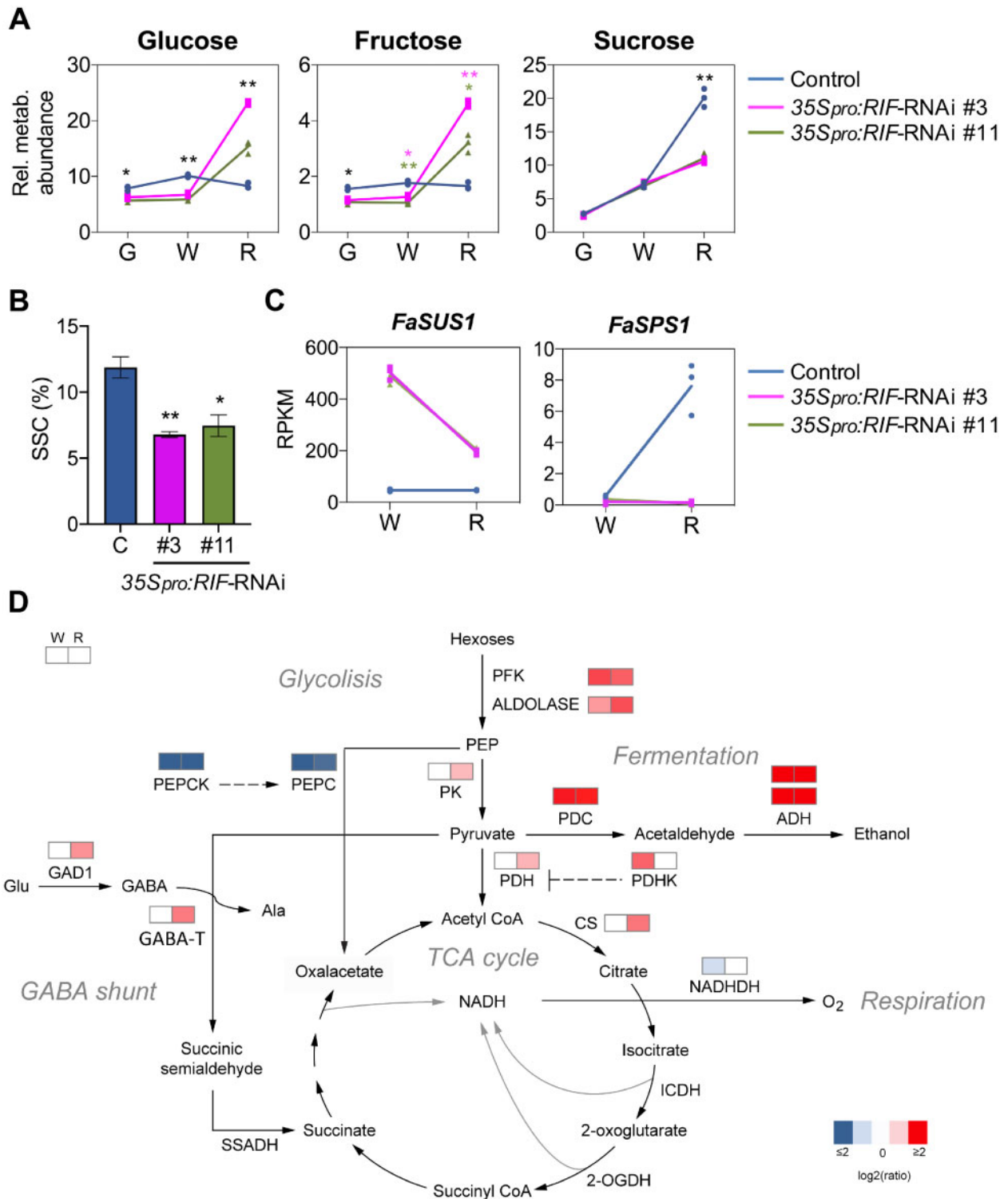
Figure 5 FaRIF contributes to the regulation of primary and energy metabolism. A, Content of main sugars in control and *35Spro:RIF*-RNAi receptacles at three ripening stages. Data are normalized to the mean response calculated for an internal control. B, Quantification of SSC. C, Expression of genes involved in sucrose metabolism supporting higher levels of glucose and fructose and lower levels of sucrose. D, Expression of genes involved in glycolysis, TCA cycle, fermentation, respiration, and GABA shunt by RNA-seq. Colors denote the average $\log_2$ fold-change of *35Spro:RIF*-RNAi/control in both transgenic lines, at the white and red stages. Red and blue show up- and downregulation, respectively, in both silenced lines. Data in (A) and (B) are from three and 10 biological replicates, respectively, analyzed by Student's t test (*$P < 0.01$; **$P < 0.001$). Colored asterisks denote significant difference for one of the RNAi lines compared with the control. G, green; W, white; R, red receptacles.

solids (soluble solid content, SSC or °Brix) in red *35Spro:RIF*-RNAi receptacles (Figure 5B). Consistent with this observation, *SUCROSE SYNTHASE1* (*FaSUS1*), which encodes the enzyme catalyzing the reversible cleavage of sucrose, was upregulated in both white and red receptacles of *35Spro:RIF*-RNAi fruits (Figure 5C). In addition, *SUCROSE PHOSPHATE SYNTHASE1* (*FaSPS1*), involved in sucrose biosynthesis, was dramatically downregulated (over 50-fold) at the red stage (Figure 5C).

Directly related to glucose and fructose metabolism, we determined that genes encoding glycolytic enzymes, such as *ATP-DEPENDENT 6-PHOSPHOFRUCTOKINASE6* (*FaPFK6*), *FRUCTOSE-BISPHOSPHATE ALDOLASE8* (*FaFBA8*), and *PYRUVATE KINASE* (*FaPK*), were upregulated in silenced fruits (Figure 5D). This result is consistent with an induced glycolytic flux, which is supported by a two-fold increase in the content of pyruvate (Supplemental Data Set S6). Pyruvate can follow different fates depending on the cellular environment, specifically energy demand and oxygen availability (Bui et al., 2019). Notably, MapMan analysis showed enrichment in genes involved in the fermentation process (Supplemental Figure S7B), such as *PYRUVATE DECARBOXYLASE1* (*FaPDC1*) and two *ALCOHOL DEHYDROGENASE* genes (*FaADHs*), which were upregulated in *35Spro:RIF*-RNAi receptacles (Figure 5D; Supplemental Table S1). Supporting an increase in anaerobic metabolism, two *ETHYLENE-RESPONSIVE FACTOR* (*ERF*) genes, *FaERF-74* and *FaERF-17* (Li et al., 2020), whose putative orthologs in Arabidopsis, *RELATED TO APETALA2 12* (*RAP2.12*) and *HYPOXIA-RESPONSIVE ERF* (*HRE2*), are positive regulators of the hypoxic response (Hinz et al., 2010; Licausi et al., 2010), were also upregulated in receptacles of RNAi lines (Supplemental Table S1). In parallel, genes involved in the tricarboxylic acid cycle were also differentially expressed, such as the genes encoding the mitochrondrion-localized enzymes PYRUVATE DEHYDROGENASE (FaPDH) and CITRATE SYNTHASE (FaCS), which were upregulated in red *35Spro:RIF*-RNAi, in agreement with the increase in the content of the tricarboxylic acid intermediates citric, 2-oxoglutaric, and malic acids (Figure 5D; Supplemental Table S1 and Figure S9B). Besides these changes, a number of genes involved in primary energetic metabolism were also differentially expressed, such as a *NADH DEHYDROGENASE* (*FaNADHDH*), *PYRUVATE DEHYDROGENASE KINASE* (*FaPDHK*), *PHOSPHOENOLPYRUVATE CARBOXYLASE* (*FaPEPC*), and *PHOSPHOENOLPYRUVATE CARBOXYLASE KINASE* (*FaPEPCK*), among other genes (Figure 5D; Supplemental Table S1), suggesting an alteration in the balance of aerobic/anaerobic metabolism in *35Spro:RIF*-RNAi fruits, a parameter that has been reported to change along with strawberry fruit ripening (Wang et al., 2017).

Genetic manipulation of *FaRIF* expression reveals its essential role in fruit development and ripening

We showed that, although *FaRIF* mRNA levels were remarkably high in receptacles, they were also rather high in achenes, reaching over 300 RPKM at the white and red-ripening stages (Figure 1B). It has been well established that communication between achenes and receptacles is important to control strawberry fruit development and ripening (Nitsch, 1950; Liao et al., 2018). Therefore, we next aimed to study the phenotypic and molecular consequences of silencing *FaRIF* specifically in the receptacle during late stages of ripening. For this purpose, we placed the expression of the *FaRIF* RNAi hairpin under the control of the *EXPANSIN2* (*FaEXP2*) promoter (*EXP2pro:RIF*-RNAi). *EXP2*, which encodes a cell-wall hydrolytic enzyme, is mostly expressed in receptacles from the turning stage (Supplemental Figure S10) (Sánchez-Sevilla et al., 2017). In addition, we also investigated the role of *FaRIF* in fruit ripening by overexpressing the *FaRIF* coding sequence (CDS) under the constitutive 35S promoter. For this purpose, we cloned the *Green Fluorescent Protein* (*GFP*) gene downstream and in-frame of the *FaRIF* CDS to generate *35Spro:RIF-GFP*.

Two out of four established stable transgenic lines for *EXP2pro:RIF*-RNAi (#1 and #7) and the only two surviving overexpressing lines (*35Spro:RIF* #1 and *35Spro:RIF-GFP* #1) were selected for further characterization (Figure 6). We failed to detect FaRIF in red receptacles of any of the two *EXP2pro:RIF*-RNAi lines selected, as determined by Immunoblot analyses, indicating efficient silencing of *FaRIF* under this promoter at the ripe stage (Figure 6B). Conversely, the overexpression lines showed a significant increase of FaRIF in red receptacles, either as a native protein (*35Spro:RIF* #1) or as a GFP-tagged protein (*35Spro:RIF-GFP* #1) (Figure 6B). In contrast to *35Spro*- and *EXP2pro*-RNAi lines, adult plants overexpressing *FaRIF* exhibited impaired plant development (Supplemental Figure S4), suggesting that the ubiquitous expression of *FaRIF* has deleterious effects.

The phenotypic analysis of ripe receptacles showed that the two *EXP2pro*-RNAi lines showed paler receptacles enriched in the yellow part of the spectrum, similar to what we observed in the 35S-RNAi lines (Figure 6A and C). Interestingly, *FaRIF* silencing from the *EXP2* promoter resulted in dark red achenes (Figure 6A) in contrast to *35Spro:RIF*-RNAi lines (Figure 2D), which is consistent with the differential silencing of *FaRIF* expected in *35Spro*- and *EXP2pro*-RNAi lines. On the contrary, *FaRIF* overexpression lines showed an opposite color phenotype for their receptacles compared with the RNAi lines (Figure 6A). The receptacles were unusually dark and enriched in the green and blue part of the spectrum (Figure 6C). Fruit firmness also followed an opposite trend when *FaRIF* was either silenced or overexpressed, since ripe *EXP2pro:RIF*-RNAi and *35Spro:RIF(-GFP)* receptacles were firmer and softer than those of the control, respectively (Figure 6C). These results confirm the role of *FaRIF* in controlling anthocyanin production and cell-wall characteristics during ripening. Surprisingly, and in contrast to *35Spro:RIF*-RNAi lines, we observed no changes for SSC in *EXP2pro*-RNAi receptacles, whereas the overexpression lines showed a lower content of soluble solids content (Figure 6C).
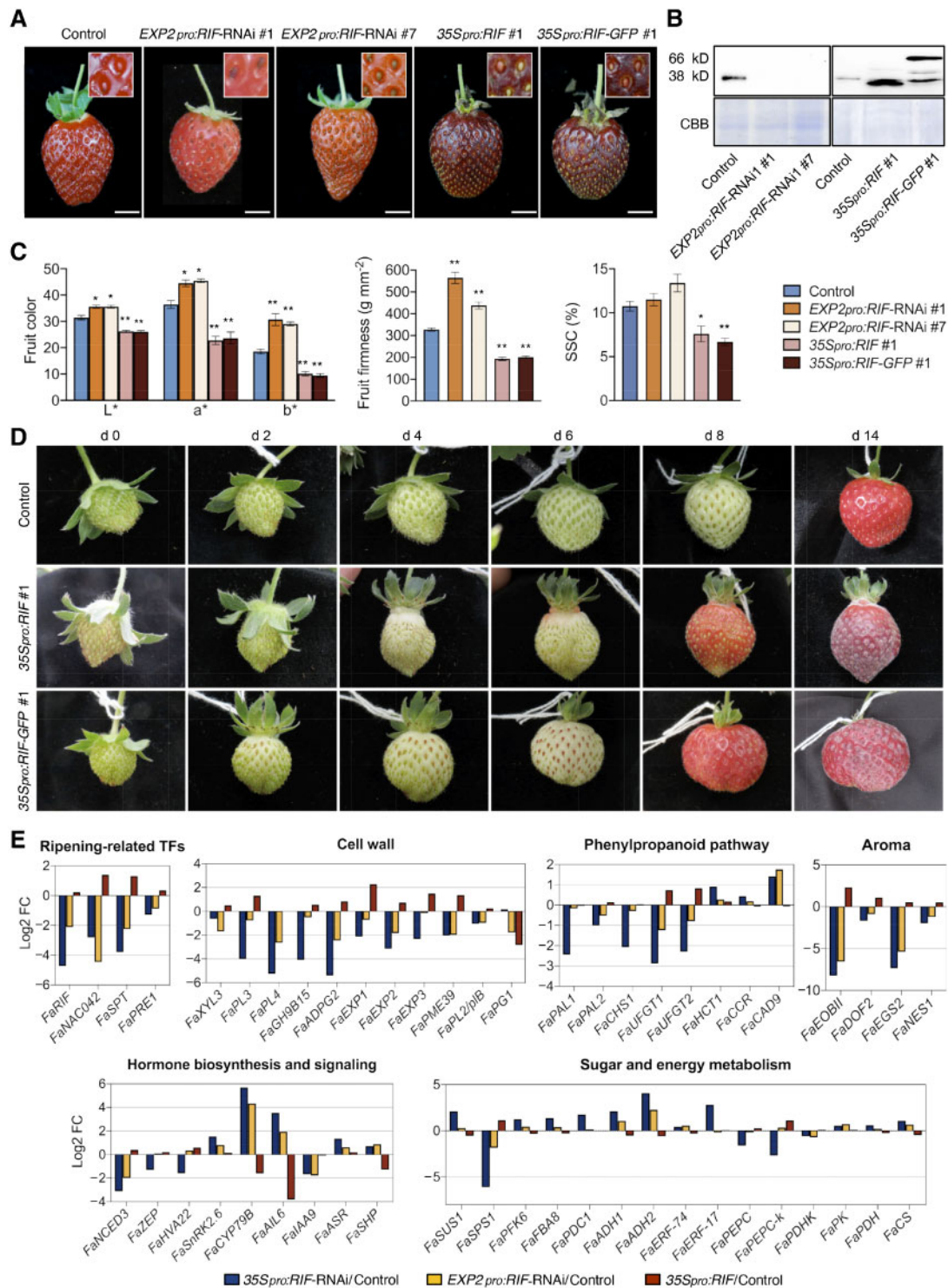
Figure 6 Effects on ripening when *FaRIF* is specifically silenced at late stages of receptacle ripening (*EXP2* promoter) or overexpressed (35S promoter). A, Fruit phenotype at the red stage in control and stable *EXP2pro:RIF*-RNAi, *35Spro:RIF* and *35Spro:RIF-GFP* transgenic lines. Inset: detail of the achenes. Scale bars, 1 cm. B, Immunoblot analysis in control and stable *EXP2pro:RIF*-RNAi, *35Spro:RIF* and *35Spro:RIF-GFP* ripe receptacles to detect native FaRIF protein (38 kD) and FaRIF–GFP fusion protein (66 kD) using anti-FaRIF antibody (upper). CBB staining of total nuclear protein extracts are shown in the (bottom) as loading control. C, Color characterization in the CIELAB color space for the lightness coefficient (L*), green-red (a*), and yellow-blue spectrum (b*) (left plot); fruit firmness measurements (middle plot); quantification of SSC (right plot). Data are means ± SE of 10 biological replicates analyzed by Student's t test (*$P < 0.05$; **$P < 0.001$). D, Representative pictures of a single fruit for control and *FaRIF* overexpression lines out of 10 analyzed showing the color progression over 14 days. Fruit size cannot be directly compared across panels. E, Log$_2$ fold-change of genes involved in different processes in *35Spro:RIF*-RNAi, *EXP2pro:RIF*-RNAi, and *35Spro:RIF*.

In order to determine whether the opposite fruit phenotype of the *FaRIF* overexpression lines is a consequence of an acceleration of the global process, we next scored the progress of fruit ripening of the overexpression lines over time, as performed previously for the *35Spro:RIF*-RNAi lines (Figure 2E). As shown in Figure 6D, overexpression of *FaRIF* was sufficient to cause a faster anthocyanin production and receptacle senescence, supporting a key role for FaRIF in controlling the fruit-ripening progress.

Finally, we performed a transcriptome analysis of receptacles of the control, *EXP2pro:RIF-RNAi* #1 and #7, and *35Spro:RIF* #1 lines at their respective ripe stages (Supplemental Data Set S1). Interestingly, many genes previously found to be differentially expressed in *35Spro:RIF*-RNAi receptacles were confirmed in the *EXP2pro*-RNAi lines, whereas displaying an opposite trend in the overexpression line. Among these genes, *FaNAC042*, and three other ripening-related TF genes, i.e., *FaEOBII*, *FaSPT*, and *FaPRE1*, were downregulated in both *35Spro-* and *EXP2pro*-RNAi lines and induced in *35Spro:RIF* #1 (Figure 6E). The opposite expression of *FaNAC042* in the RNAi and the overexpression line support the role of FaRIF in promoting *FaNAC042* expression. Consistent with the higher and lower firmness that the RNAi and overexpression receptacles displayed, respectively (Figures 3, B and 6, C), genes involved in cell-wall degradation and modification showed a remarkable opposite trend, being mainly downregulated with both RNAi strategies, but upregulated in the overexpression line (Figure 6E). This opposite pattern was also seen for genes in the phenylpropanoid pathway, as expected based on the different color of the receptacle shown by the RNAi and the overexpression lines (Figures 2, D and 6, A), and for genes involved in the production of volatiles, phytohormone biosynthesis and signaling, and sugar and energy metabolism (Figure 6E). Thus, all these data support the role of FaRIF as a key regulator of strawberry fruit ripening.

DISCUSSION

A number of TFs that regulates different and specific aspects of strawberry fruit ripening have been characterized to date (Aharoni et al., 2001; Lin-Wang et al., 2010; Seymour et al., 2011). Out of the 112 *NAC* genes identified in *F. vesca* (Moyano et al., 2018), 10 showed increases in their mRNA levels during ripening (Moyano et al., 2018; Sánchez-Sevilla et al., 2017) (Figure 1A). Among them, only *FcNAC1*, the ortholog to *NAC022* in *F. chiloensis*, has been characterized in relation to strawberry ripening. The authors identified cis-regulatory elements able to respond to some phytohormones and reported that *FcNAC1* expression is regulated by ABA and auxin (Carrasco-Orellana et al., 2018). However, no functional analysis for any ripening-related NAC TF has been described in strawberry. In the present study, we functionally characterized *FaNAC035* (*FaRIF*). Phenotypic and molecular analyses of *FaRIF*-RNAi and *FaRIF*-overexpression lines showed that FaRIF is key to promote ripening of strawberry fruits through regulating phytohormone biosynthesis

and signaling, ripening-related TFs, energy metabolism, and specific processes such as cell-wall remodeling, the phenylpropanoid pathway, and sugar content.

The involvement of different phytohormones on the strawberry fruit growth and ripening processes has been well established (Symons et al., 2012; Gu et al., 2019). The early stages of strawberry receptacle development are controlled by auxin and GAs that are synthesized in achenes (Nitsch, 1950; Csukasi et al., 2011). Therefore, in these early stages, achene-receptacle communication is essential. At later stages, the ripening of the receptacle is dependent on a decrease in auxin content and a local biosynthesis of ABA (Jia et al., 2011; Liao et al., 2018). Nevertheless, regulatory factors controlling these phytohormones remain elusive. Our analyses indicate that *FaRIF* regulates genes involved in phytohormone biosynthesis and signaling, suggesting a regulatory role in phytohormone cross-talk to promote strawberry fruit development and ripening. Indeed, our results showed that FaRIF promotes ABA biosynthesis by the induction of *FaNCED3* and *FaZEP*. The recovery of the ripening process in *35Spro:RIF*-RNAi fruits treated with an exogenous application of ABA shows that FaRIF acts upstream of ABA (Figure 4C). Conversely, it was reported that the transcript levels of *FaRIF* are substantially diminished after application of 1-nordihydroguaiaretic acid, an inhibitor of ABA biosynthesis (Moyano et al., 2018), revealing that *FaRIF* expression is positively regulated by ABA. Thus, we propose that *FaRIF* and ABA may act in a positive regulatory feedback loop to promote strawberry fruit ripening. This regulatory mechanism is documented in other systems such as seedling photomorphogenesis, whereby an NAC TF (ATAF2) and brassinosteroids are involved in a feedback regulation loop (Peng et al., 2015).

ABA controls anthocyanin biosynthesis in strawberry fruits (Jia et al., 2011, 2016). Interestingly, we observed differential progression in the color of receptacles and achenes of *RIF*-RNAi lines under either the *35S* or the *EXP2* promoters (Figure 6A), indicating that FaRIF is also important to induce anthocyanin biosynthesis in achenes and that it controls the biosynthesis in receptacles independently of achene development.

One of the main processes associated with strawberry fruit ripening is the loss of firmness of receptacles due to the activity of cell-wall remodeling enzymes (Posé et al., 2011). Our transcriptome analyses indicate that FaRIF positively regulates many genes involved in cell-wall disassembly (Figures 3, A and 6, E), although other cell-wall-related genes were upregulated in the RNAi lines (Supplemental Figure S8A). Therefore, although we cannot predict the specific effects of *FaRIF* silencing on cell-wall structure or composition, the altered firmness of the fruits in both the *FaRIF*-RNAi and overexpression lines supports a general role for FaRIF in cell-wall degradation and the loss of firmness during ripening. Besides cell-wall composition, the degree of lignification is also associated with firmness in many fleshy fruits (Li et al., 2010). Our data showed that *FaRIF* represses genes from the monolignol pathway, consistent with the increased

lignin accumulation observed in *35Spro:RIF*-RNAi fruits (Figures 3, C and 6, E). Therefore, *FaRIF* plays a key role in promoting fruit softening by regulating cell-wall remodeling enzymes and lignin content.

The regulation of central metabolic fluxes is essential during fruit development (Centeno et al., 2011; Colombié et al., 2015). In strawberry fruits, the expression of *NADHDH* genes peaks between the white and the red fruit stages during ripening (Sánchez-Sevilla et al., 2017), suggesting an increase in respiration at this transition. It has also been reported that the glycolytic pathway is inhibited during ripening and that arresting respiration through the silencing of subunit alpha of the pyruvate dehydrogenase gene *PDHE1α* accelerates the ripening process. These studies indicate that the anaerobic/aerobic balance of the energy metabolism is programmed along with strawberry fruit ripening (Wang et al., 2017; Luo et al., 2020). Our transcriptome data showed that *FaRIF* participates in the control of this balance, as reflected by the changes in mRNA levels of metabolic genes of anaerobic pathways such as glycolysis and fermentation, aerobic pathways like the TCA cycle and respiration as well as genes from the anaplerotic pathways PEPC/PEPCK and the γ-aminobutyric acid (GABA) shunt (Figures 5, D and 6, E). Furthermore, metabolic changes observed in the *35Spro:RIF*-RNAi lines, such as the accumulation of glucose, fructose, raffinose, galactinol, *myo*-inositol, proline, and TCA intermediates, are characteristics of a hypoxia-like response (Banti et al., 2013). All these data point to FaRIF as an important regulator of the onset of aerobic metabolism that occurs during strawberry fruit ripening.

There is a local sucrose metabolism in fruits, whereby the enzymes SPS and SUS, and the recently identified protein kinase FaSnRK1a, play essential roles (Miron and Schaffer, 2005). *35Spro:RIF*-RNAi receptacles showed lower content of sucrose and a reduced SSC. Transcriptome analysis showed that *FaRIF* promotes sucrose accumulation during ripening, likely by regulating the expression of *FaSPS1* and *FaSUS*. Surprisingly, SSC was also reduced in *RIF* overexpression lines, despite showing an opposite transcript accumulation pattern for these metabolic genes and a remarkable acceleration of ripening processes such as coloration and loss of firmness (Figure 6, C and D). This result might be explained by a slower progress in sucrose accumulation compared with that of anthocyanin and cell-wall degradation during the ripening process. Thus, the red *35Spro:RIF*(-GFP) receptacles might be delayed in terms of sucrose composition, despite their advanced color and firmness. In contrast, despite the similar ripening phenotype seen in *EXP2pro*-RNAi and *35Spro*-RNAi lines, we observed no differences in SSC in ripe *EXP2pro:RIF*-RNAi receptacles relative to controls (Figure 6C). Since *FaRIF* was silenced in the late stages of ripening in the *EXP2pro*-RNAi lines, we hypothesize that *FaRIF* is important to control sucrose accumulation during ripening from early stages of development.

The phylogenetic analysis of FaRIF protein showed that it is closely related to NACs involved in senescence. Among them, the redundant Arabidopsis *NARS1/NAC* and *NARS2/NAM* genes have been shown to regulate embryogenesis and, interestingly, silique senescence (Kunieda et al., 2008). Furthermore, the phylogenetic analysis also revealed the homology between FaRIF and SlNOR, a TF previously reported to control tomato fruit ripening (Giovannoni, 2004; Wang et al., 2019). Besides, it has been reported that MdNAC18.1, the ortholog to SlNOR in apple, regulates apple fruit ripening by controlling fruit firmness and harvest time (Migicovsky et al., 2016; Yeats et al., 2019). Thus, all these data support a role for these NAC TFs in the regulation of ripening not only in both dry and fleshy fruits but also in organs with different ontogenetic origins such as the tomato fruit and false fruits such as apple (pome) and strawberry (achenetum).

In summary, we show that the NAC TF FaRIF plays a central role in controlling strawberry fruit ripening. Its regulatory role is executed from the early stages of fruit development, contributing to the crosstalk among different phytohormones through fruit growth and ripening, and to basic processes of fruit development such as the balance between anaerobic/aerobic metabolism. In addition, the delayed ripening phenotype of *FaRIF*-silenced fruits, characterized by an increased fruit firmness and extended life, opens the door to investigating the phenotypic consequences of different levels of *FaRIF* expression, and their potential application in extending fruit shelf-life in strawberry breeding programs. Although the constitutive silencing of *FaRIF* reduced SSC in ripe fruits, a late modulation of its expression, such as that seen in the *EXP2pro*-RNAi lines, might result in improved fruit firmness without changes in the sugar content.

Materials and methods

Cloning of *FaRIF* and phylogenetic studies

The full-length CDS for FvH4_3g20700 in *F. × ananassa* (*FaNAC035*, named *FaRIF* in this work) was obtained from cDNA generated from ripe *F. × ananassa* cv. Camarosa fruits using P13 and P14 oligonucleotides (Supplemental Table S2).

Multiple sequence alignment of NAC proteins was performed using MUSCLE with the Seaview version 4 software (Gouy et al., 2010). The phylogenetic tree was inferred by the neighbor-joining method. A total of 1,000 bootstrap pseudo-replicates were used to estimate the reliability of internal nodes. Evolutionary distances were computed using the Poisson correction method. Tree inference was performed using MEGA version 7 (Kumar et al., 2016). The dataset comprised 112 previously reported NAC proteins obtained from Genbank (see Accession numbers section and Moyano et al., 2018).

DNA sequence alignment was performed using the Clustal Omega program (https://www.ebi.ac.uk/Tools/msa/clustalo/).

Plasmids construction

All oligonucleotides used for plasmid construction are listed in Supplemental Table S2. All PCR reactions were performed

using iProof™ high-fidelity DNA polymerase (Bio-Rad), and the constructs were verified by Sanger sequencing.

The intron-containing hairpin RNA (ihpRNA) 35Spro:RIF-RNAi construct was generated using a 265-bp fragment of FaRIF (nts 678–942 from the ATG codon), amplified from cDNA prepared from red fruits using primers P649 and P650, which incorporate two restriction sites used for cloning into the pHANNIBAL vector. The ihpRNA fragment cloned in pHANNIBAL was then introduced into the pBINPLUS binary vector using SacI/NheI and SacI/XbaI restriction sites, respectively, obtaining the final pBINPLUS-35Spro:RIF-RNAi construct. The ihpRNA EXP2pro:RIF-RNAi construct was generated using the same 265-bp FaRIF fragment amplified from the 35Spro:RIF-RNAi construct and the EXP2pro:GUS-GFP construct (pKGWFS7 backbone) (Schaart et al., 2011). To generate the FaRIF overexpression constructs pCM23 (35Spro:RIF) and pCM24 (35Spro:RIF-GFP), the full FaRIF CDS was amplified from cDNA prepared from red fruits using primers P8 and P13. The PCR products were first cloned into pCR8/GW/TOPO vectors (Life Technologies) to create pCM9 and pCM10, respectively, which were recombined through LR reaction (Gateway) into the pK7WG2D and pK7WG2 binary vectors, respectively, resulting in pCM23 and pCM24.

Plant materials and stable transformation

F. × ananassa cv. Camarosa control and transgenic strawberry adult plants were grown and maintained in a shading house (IFAPA, Churriana, Málaga, Spain) and greenhouse under natural sunlight (IHSM, Málaga, Spain) conditions, using a mixture of universal substrate and river sand (3:1 [v/v]). In vitro plants were grown in phytotrons under cool-white light (at 15 µE) with a long-day photoperiod (16-h light/8-h dark) at 22°C.

For stable transformation of F. × ananassa cv. Camarosa, plants were micropropagated in N30K medium supplemented with 2.2 µM kinetin. Transformation was performed according to the protocol described by Barceló et al. (1998). Strawberry leaf discs were transformed with Agrobacterium (Agrobacterium tumefaciens) strain LBA4404 harboring the constructs described above. Regenerated shoots were selected on the same medium supplemented with 50 mg L^{-1} kanamycin and 500 mg L^{-1} carbenicillin.

Fruit phenotypic analysis

35Spro:RIF-RNAi lines were evaluated during three consecutive growing seasons, and EXP2pro-RNAi and overexpression lines during two. Non-transformed cv. Camarosa plants were used as control. At least 10 fruits for each control and transgenic lines were harvested at the stage of full ripeness. The external color of the fruit was analyzed using the Color reader CR-10 PLUS (KONICA MINOLTA, Ramsey, NJ, USA). For fruit firmness, two measures on each side of the fruit were performed using a penetrometer (Effegi FDP500) with a 3-mm diameter cylinder needle. SSC or °Brix was measured with a digital refractometer (ATAGO PR32).

Evaluation of fruit ripening progress

Ten fruits from each line (control, 35Spro:RIF-RNAi, 35Spro:RIF, and 35Spro:RIF-GFP) were labeled at the same early green stage (Day 0), and the fruit phenotype was monitored every day for 30 days (35Spro:RIF-RNAi) or 14 days (overexpression lines). Percentage of 35Spro:RIF-RNAi fruits at seven different ripening stages (green, green/white, white, white/turning, turning, red, and overripe) was calculated at d 1, 10, 15, and 24.

Gene expression analysis by RT-qPCR

Total RNA was isolated as previously described (Gambino et al., 2008) from three biological replicates of receptacles after the removal of achenes for the control and transgenic lines. Each biological replicate consisted of three technical replicates of five receptacles. One microgram of total RNA was DNase I-treated (TURBO™ DNAse, Invitrogen) and first-strand cDNA was synthesized using oligo(dT) ant the iScript cDNA Synthesis kit (Bio-Rad). The resulting first-strand cDNA was diluted 25-fold and 4 µL was used as a template. Quantitative PCR was performed using SsoFast EvaGreen® Supermix (Bio-Rad) and specific oligonucleotides (Supplemental Table S2) on a CFX96™ Real-Time System (Bio-Rad). Relative expression values were calculated by $\Delta\Delta C_t$ method using FaCHP1 as the reference gene for the RT-qPCR normalization (Clancy et al., 2013) (Supplemental Table S2).

Protein extraction and immunoblot analysis

Receptacles after the removal of achenes of control fruits at the green, white, turning, and red stages, and from control and transgenic fruits at the state of full ripeness were used for this analysis. Nuclear protein extraction was performed as previously described (Bouyer et al., 2011). The proteins were separated on 10% sodium dodecyl sulphate–polyacrylamide gel electrophoresis SDS–PAGE and electroblotted using Tran-Blot Turbo Transfer System (Bio-Rad) onto polyvinylidene difluoride (PVDF) membranes (Immobilon-P, Millipore) following the manufacturer's protocol. The membranes were blocked using 30 mL of blocking solution (5% fat-free powdered milk in Tris-buffered saline with 0.05% Tween-20 [TBST]) for 2 h. Then, the membranes were washed with TBST and incubated with the anti-RIF antibody (1:50 dilution) overnight. The anti-RIF antibody was designed using a FaRIF 15-amino acid peptide (amino acids 268–282 from Met: C-PNLYWNHDQEDEAGL-NH₂) and generated by Eurogentec, S.A. Liége Science Park (Belgium). The secondary antibody used in this study was anti-Rabbit IgG whole molecule-HRP conjugate (1:14,000; A-0545, Sigma). Signal was detected using Clarity ECL Western Blotting Substrates (Bio-Rad) or SuperSignal West Femto Maximum Sensitivity Substrate (ThermoFisher). The images were acquired using the Chemidoc XRS + System (Bio-Rad). SDS–PAGE and immunoblotted PVDF membranes were stained with Coomassie Brilliant Blue (CBB) R 250 to confirm equal loading between the different samples.

Transcriptome analysis by RNA-seq

RNA-seq and primary and secondary metabolome analyses were carried out using the same samples. Each biological replicate comprised a minimum of 20 receptacles. The RNA quality and concentration were validated and measured on a Bioanalyzer 2100 (Agilent Technologies Santa Clara, CA, USA), and the RNA integrity number values were >8.0 for all biological replicates. Strand specific mRNA libraries were generated for *35Spro:RIF-RNAi* and their respective control samples as described by Zhong et al. (2011). Paired-end Illumina mRNA libraries were generated for *EXP2pro:RIF-RNAi*, *35Spro:RIF*, and their respective control samples using the TruSeq stranded mRNA according to the manufacturer's instructions (Illumina Inc., San Diego, CA, USA). Libraries from *35Spro:RIF-RNAi* and their respective controls were sequenced on an Illumina HiSeq2000 platform, and those from *EXP2pro:RIF-RNAi*, *35Spro:RIF* and their respective controls on a NextSeq550 platform, generating 100-bp single-end and 2×75-bp paired-end reads, respectively. Raw sequences were trimmed and mapped against using the assembly and annotation version v4.0.a1 of the *F. vesca* reference genome (https://www.rosacea.org/species/fragaria_vesca/genome_v4.0.a1; Edger et al., 2018), a high-quality reference genome, using CLC Genomics Workbench 9 (https://www.qiagenbioinformatics.com/products/clc-main-workbench/). MapMan bins were used for assignment of DEGs to functional categories (Usadel et al., 2009).

Metabolome analysis

Primary and secondary metabolites were analyzed as described by Vallarino et al. (2018). For primary metabolites, the identification of metabolites was based on cross-reference with the Golm Database (Kopka et al., 2005). For secondary metabolites, putative identification and annotation were performed using literature, mainly from strawberry. Here, the data are presented as peak response in mass chromatograms and represented as a direct fraction of peak area. No quantitative standards were used in this study. ABA analysis by Gas Chromatography Time-Of-Flight Mass Spectrometry (GC–TOF–MS) was carried out according to Vallarino et al. (2019).

Lignin staining

Lignified tissues were visualized using Weisner staining (Phloroglucinol-HCl, Sigma-Aldrich) (Clifford, 1974). This stain reacts with aldehyde groups in lignin, giving a characteristic deep reddish-purple coloration to the xylem in vascular bundles. In detail, fruits at the red stage were cut in slices and incubated in 1% phloroglucinol in a 70% (v/v) ethanol solution until they were totally cleared. Then the phloroglucinol solution was removed, and a few drops of 37% (v/v) HCl were added. The lignified tissues appeared with a pink-red coloration about 5 min later. Pictures were taken immediately since color faded in around 30 min.

ABA treatment

Mock solution consisting of 2% (v/v) ethanol and 100 μM ABA (in 2% ethanol) were infiltrated in green fruits as previously described by Li et al. (2019). Five replicates per condition and genotype were used.

Accession numbers

Sequence data from this article can be found in Supplemental Tables S3 and S4.

RNA-seq datasets were deposited at the Gene Expression Omnibus at NCBI under the accession number GSE167107.

Supplemental Data

The following materials are available in the online version of this article.

Supplemental Figure S1. Phylogenetic analysis of NAC proteins.

Supplemental Figure S2. Alignment of NAC proteins.

Supplemental Figure S3. Phenotype of ripe strawberries in control, and four independent stable *35Spro:RIF-RNAi* lines.

Supplemental Figure S4. Representative phenotypes of adult plants of the control and the different transgenic lines used in this work.

Supplemental Figure S5. Global transcriptome analysis in control and *35Spro:RIF-RNAi* receptacles.

Supplemental Figure S6. Alignment of *FaRIF* RNAi hairpin with *FaNAC042* homologous sequences.

Supplemental Figure S7. MapMan enrichment analysis.

Supplemental Figure S8. Expression of cell-wall and aroma-related genes in receptacles of control and *35Spro:RIF-RNAi* fruits.

Supplemental Figure S9. Secondary and primary metabolism in receptacles of control and *35Spro:RIF-RNAi* fruits.

Supplemental Figure S10. Expression of *FaEXP2* at four ripening stages of receptacles and achenes.

Supplemental Data S1. DNA and protein sequence of *FaRIF*/FaRIF.

Supplemental Table S1. List of common DEGs in *35Spro:RIF-RNAi* #3 and #11.

Supplemental Table S2. List of oligonucleotides used in this study.

Supplemental Table S3. *F. vesca* ID numbers of genes mentioned in this work.

Supplemental Table S4. GenBank accession numbers.

Supplemental File 1. Alignment of the NAC proteins included in the phylogenetic tree.

Supplemental File 2. Newick format of the alignment shown in Supplemental File 1.

Supplemental Data Set S1. Transcriptome analysis in receptacles of control and *35Spro:RIF-RNAi*, *EXP2pro:RIF-RNAi* and *35Spro:RIF* lines.

Supplemental Data Set S2. List of common DEGs in the two *35Spro:RIF-RNAi* lines in both white and red stages of the receptacle ripening.

Supplemental Data Set S3. Expression data of differentially expressed *FaNAC* transcription factors and *NCEDs* in control and *35Spro:RIF*-RNAi lines at white and red stages of receptacle ripening.

Supplemental Data Set S4. MapMan bins enrichment analysis.

Supplemental Data Set S5. Secondary metabolism analysis in control and *35Spro:RIF*-RNAi lines at three ripening stages.

Supplemental Data Set S6. Primary metabolism analysis in control and *35Spro:RIF*-RNAi lines at three ripening stages.

Supplemental Data Set S7. Summary of statistical analyses.

References

Aharoni A, De Vos CH, Wein M, Sun Z, Greco R, Kroon A, Mol JN, O'Connell AP (2001) The strawberry FaMYB1 transcription factor suppresses anthocyanin and flavonol accumulation in transgenic tobacco. Plant J **28**: 319–332

Aharoni A, Giri AP, Verstappen FWA, Bertea CM, Sevenier R, Sun Z, Jongsma MA, Schwab W, Bouwmeester HJ (2004) Gain and loss of fruit flavor compounds produced by wild and cultivated strawberry species. Plant Cell **16**: 3110–3131

Bai M, Sun J, Liu J, Ren H, Wang K, Wang Y, Wang C, Dehesh K (2019) The B-box protein BBX19 suppresses seed germination via induction of ABI5. Plant J **99**: 1192–1202

Banti V, Giuntoli B, Gonzali S, Loreti E, Magneschi L, Novi G, Paparelli E, Parlanti S, Pucciariello C, Santaniello A, Perata P (2013) Low oxygen response mechanisms in green organisms. Int J Mol Sci **14**: 4734–4761

Barceló M, Mansouri EII, Mercado J-Á, Quesada MA, Pliego-Alfaro F (1998) Regeneration and transformation via *Agrobacterium tumefaciens* of the strawberry cultivar Chandler. Plant Cell Tissue Organ Culture **54**: 29–36

Benítez-Burraco A, Blanco-Portales R, Redondo-Nevado J, Bellido ML, Moyano E, Caballero JL, Muñoz-Blanco J (2003) Cloning and characterization of two ripening-related strawberry (*Fragaria × ananassa* cv. Chandler) pectate lyase genes. J Exp Bot **54**: 633–645

Bouyer D, Roudier F, Heese M, Andersen ED, Gey D, Nowack MK, Goodrich J, Renou J-P, Grini PE, Colot V, Schnittger A (2011)

Polycomb repressive complex 2 controls the embryo-to-seedling phase transition. PLoS Genet **7**: e1002014

Bui LT, Novi G, Lombardi L, Iannuzzi C, Rossi J, Santaniello A, Mensuali A, Corbineau F, Giuntoli B, Perata P, et al. (2019) Conservation of ethanol fermentation and its regulation in land plants. J Exp Bot **70**: 1815–1827

Carrasco-Orellana C, Stappung Y, Mendez-Yañez A, Allan AC, Espley RV, Plunkett BJ, Moya-Leon MA, Herrera R (2018) Characterization of a ripening-related transcription factor FcNAC1 from *Fragaria chiloensis* fruit. Sci Rep **8**: 10524

Castillejo C, Waurich V, Wagner H, Ramos R, Oiza N, Muñoz P, Triviño JC, Caruana J, Liu Z, Cobo N, et al. (2020) Allelic variation of *MYB10* is the major force controlling natural variation in skin and flesh color in strawberry (Fragaria spp.) Fruit. Plant Cell **32**: 3723–3749

Centeno DC, Osorio S, Nunes-Nesi A, Bertolo ALF, Cameiro RT, Araújo WL, Steinhauser MC, Michalska J, Rohrmann J, Geigenberger P, et al. (2011) Malate plays a crucial role in starch metabolism, ripening, and soluble solid content of tomato fruit and affects postharvest softening. Plant Cell **23**: 162–184

Chai Y-M, Zhang Q, Tian L, Li C-L, Xing Y, Qin L, Shen Y-Y (2012) Brassinosteroid is involved in strawberry fruit ripening. Plant Growth Regul **69**: 63–69

Chen H, Zhang J, Neff MM, Hong S-W, Zhang H, Deng XW, Xiong L (2008) Integration of light and abscisic acid signaling during seed germination and early seedling development. Proc Natl Acad Sci U S A **105**: 4495–4500

Clancy MA, Rosli HG, Chamala S, Barbazuk WB, Civello PM, Folta KM (2013) Validation of reference transcripts in strawberry (Fragaria spp.). Mol Genet Genom **288**: 671–681

Clifford MN (1974) Specificity of acidic phloroglucinol reagents. J Chromatogr **94**: 321–324

Colombié S, Nazaret C, Bénard C, Biais B, Mengin V, Solé M, Fouillen L, Noubhani MD, Mazat JP, Beauvoit B, et al. (2015) Modelling central metabolic fluxes by constraint-based optimization reveals metabolic reprogramming of developing *Solanum lycopersicum* (tomato) fruit. Plant J **81**: 24–39

Concha CM, Figueroa NE, Poblete LA, Oñate FA, Schwab W, Figueroa CR (2013) Methyl jasmonate treatment induces changes in fruit ripening by modifying the expression of several ripening genes in *Fragaria chiloensis* fruit. Plant Physiol Biochem **70**: 433–444

Csukasi F, Osorio S, Gutierrez JR, Kitamura J, Giavalisco P, Nakajima M, Fernie AR, Rathjen JP, Botella MA, Valpuesta V, et al. (2011) Gibberellin biosynthesis and signalling during development of the strawberry receptacle. New Phytol **191**: 376–390

Daminato M, Guzzo F, Casadoro G (2013) A SHATTERPROOF-like gene controls ripening in non-climacteric strawberries, and auxin and abscisic acid antagonistically affect its expression. J Exp Bot **64**: 3775–3786

de Oliveira TM, Cidade LC, Gesteira AS, Filho MAC, Filho WSS, Costa MG (2011) Analysis of the NAC transcription factor gene family in citrus reveals a novel member involved in multiple abiotic stress responses. Tree Genet Genom **7**: 1123–1134

Dotto MC, Martínez GA, Civello PM (2006) Expression of expansin genes in strawberry varieties with contrasting fruit firmness. Plant Physiol Biochem **44**: 301–307

Edger PP, VanBuren R, Colle M, Poorten TJ, Wai CM, Niederhuth CE, Alger EI, Ou S, Acharya CB, Wang J, et al. (2018) Single-molecule sequencing and optical mapping yields an improved genome of woodland strawberry (*Fragaria vesca*) with chromosome-scale contiguity. Gigascience **7**: 1–7

Estrada-Johnson E, Csukasi F, Pizarro CM, Vallarino JG, Kiryakova Y, Vioque A, Merchante C, Brumos J, Medina-Escobar N, Botella MA, et al. (2017) Transcriptomic analysis in strawberry fruits reveals active auxin biosynthesis and signaling in the ripe receptacle. Front Plant Sci **8**: 889

Fait A, Hanhineva K, Beleggia R, Dai N, Rogachev I, Nikiforova VJ, Fernie AR, Aharoni A (2008) Reconfiguration of the achene and

receptacle metabolic networks during strawberry fruit development. Plant Physiol 148: 730–750

Gambino G, Perrone I, Gribaudo I (2008) A Rapid and effective method for RNA extraction from different tissues of grapevine and other woody plants. Phytochem Anal 19: 520–525

Giovannoni JJ (2004) Genetic regulation of fruit development and ripening. Plant Cell 16 (Suppl): S170–S80

Gouy M, Guindon S, Gascuel O (2010) SeaView version 4: A multi-platform graphical user interface for sequence alignment and phylogenetic tree building. Mol Biol Evol 27: 221–224

Gu T, Jia S, Huang X, Wang L, Fu W, Huo G, Gan L, Ding J, Li Y (2019) Transcriptome and hormone analyses provide insights into hormonal regulation in strawberry ripening. Planta 250: 145–162

Guo J, Wang S, Yu X, Dong R, Li Y, Mei X, Shen Y (2018) Polyamines Regulate Strawberry Fruit Ripening by Abscisic Acid, Auxin, and Ethylene. Plant Physiol 177: 339–351

Guo Y, Gan S (2006) AtNAP, a NAC family transcription factor, has an important role in leaf senescence. Plant J. 46: 601–612

Han Y, Dang R, Li J, Jiang J, Zhang N, Jia M, Wei L, Li Z, Li B, Jia W (2015) SUCROSE NONFERMENTING1-RELATED PROTEIN KINASE2.6, an ortholog of OPEN STOMATA1, is a negative regulator of strawberry fruit development and ripening. Plant Physiol 167: 915–930

Härtl K, Denton A, Franz-Oberdorf K, Hoffmann T, Spornraft M, Usadel B, Schwab W (2017) Early metabolic and transcriptional variations in fruit of natural white-fruited. Sci Rep 7: 45113

Hinz M, Wilson IW, Yang J, Buerstenbinder K, Llewellyn D, Dennis ES, Sauter M, Dolferus R (2010) Arabidopsis RAP2.2: an ethylene response transcription factor that is important for hypoxia survival. Plant Physiol 153: 757–772

Jia H, Jiu S, Zhang C, Wang C, Tariq P, Liu Z, Wang B, Cui L, Fang J (2016) Abscisic acid and sucrose regulate tomato and strawberry fruit ripening through the abscisic acid-stress-ripening transcription factor. Plant Biotechnol J 14: 2045–2065

Jia H, Wang Y, Sun M, Li B, Han Y, Zhao Y, Li X, Ding N, Li C, Ji W, Jia W (2013) Sucrose functions as a signal involved in the regulation of strawberry fruit development and ripening. New Phytol 198: 453–465

Jia H-F, Chai Y-M, Li C-L, Lu D, Luo J-J, Qin L, Shen Y-Y (2011) Abscisic acid plays an important role in the regulation of strawberry fruit ripening. Plant Physiol 157: 188–199

Jiménez-Bermúdez S, Redondo-Nevado J, Muñoz-Blanco J, Caballero JL, López-Aranda JM, Valpuesta V, Pliego-Alfaro F, Quesada MA, Mercado JA (2002) Manipulation of strawberry fruit softening by antisense expression of a pectate lyase gene. Plant Physiol 128: 751–759

Kanayama Y (2017) Sugar metabolism and fruit development in the tomato. Hort J 86: 417–425

Kang C, Darwish O, Geretz A, Shahan R, Alkharouf N, Liu Z (2013) Genome-scale transcriptomic insights into early-stage fruit development in woodland strawberry Fragaria vesca. Plant Cell 25: 1960–1978

Kopka J, Chauer N, Krueger S, Birkemeyer C, Usadel B, Bergmüller E, Dörmann P, Weckwerth W, Gibon Y, Stitt M, et al. (2005) GMD@CSB.DB: the Golm Metabolome Database. Bioinformatics 21: 1635–1638

Kou X, Liu C, Han L, Wang S, Xue Z (2016) NAC transcription factors play an important role in ethylene biosynthesis, reception and signaling of tomato fruit ripening. Mol Genet Genom 291: 1205–1217

Krizek BA, Bequette CJ, Xu K, Blakley IC, Fu ZQ, Stratmann JW, Loraine AE (2016) RNA-Seq links the transcription factors AINTEGUMENTA and AINTEGUMENTA-LIKE6 to cell wall remodeling and plant defense pathways. Plant Physiol 171: 2069–2084

Kumar S, Stecher G, Tamura K (2016) MEGA7: molecular evolutionary genetics analysis Version 7.0 for bigger datasets. Mol Biol Evol 33: 1870–1874

Kunieda T, Mitsuda N, Ohme-Takagi M, Takeda S, Aida M, Tasaka M, Kondo M, Nishimura M, Hara-Nishimura I (2008) NAC family proteins NARS1/NAC2 and NARS2/NAM in the outer integument regulate embryogenesis in Arabidopsis. Plant Cell 20: 2631–2642

Li D, Mou W, Luo Z, Li L, Limwachiranon J, Mao L, Ying T (2016) Developmental and stress regulation on expression of a novel miRNA, Fan-miR73, and its target ABI5 in strawberry. Sci Rep 6: 28385

Li D, Mou W, Xia R, Li L, Zawora C, Ying T, Mao L, Liu Z, Luo Z (2019) Integrated analysis of high-throughput sequencing data shows abscisic acid- responsive genes and miRNAs in strawberry receptacle fruit ripening. Hortic Res 6: 1–13

Li X, Xu C, Korban SS, Chen K (2010) Regulatory mechanisms of textural changes in ripening fruits. Crit Rev Plant Sci 29: 222–243

Li Z, Hong Y, Chen C, Wang Z, Zheng A, Chen J, Chen Q (2020) Genome-wide identification and analysis of the AP2/ERF gene family in Fragaria vesca. Res Square 10.21203/rs.2.16253/v1

Liao X, Li M, Liu B, Yan M, Yu X, Zi H, Liu R, Yamamuro C (2018) Interlinked regulatory loops of ABA catabolism and biosynthesis coordinate fruit growth and ripening in woodland strawberry. Proc Natl Acad Sci U S A 115: E11542–E11550

Licausi F, van Dongen JT, Giuntoli B, Novi G, Santaniello A, Geigenberger P, Perata P (2010) HRE1 and HRE2, two hypoxia-inducible ethylene response factors, affect anaerobic responses in Arabidopsis thaliana. Plant J 62: 302–315

Lin-Wang K, Bolitho K, Grafton K, Kortstee A, Karunairetnam S, McGhie TK, Espley RV, Hellens RP, Allan AC (2010) An R2R3 MYB transcription factor associated with regulation of the anthocyanin biosynthetic pathway in Rosaceae. BMC Plant Biol 10: 50

Liu Z, Ma H, Jung S, Main D, Guo L (2020) Developmental mechanisms of fleshy fruit diversity in rosaceae. Annu Rev Plant Biol 71: 547–573

Luo Y et al. (2020). ABA and sucrose co-regulate strawberry fruit ripening and show inhibition of glycolysis. Mol Genet Genom 295: 421–438

Medina-Puche L, Cumplido-Laso G, Amil-Ruiz F, Hoffmann T, Ring L, Rodríguez-Franco A, Caballero JL, Schwab W, Muñoz-Blanco J, Blanco-Portales R (2013) MYB10 plays a major role in the regulation of flavonoid/phenylpropanoid metabolism during ripening of Fragaria × ananassa fruits. J Exp Bot 65: 401–417

Medina-Puche L, Martínez-Rivas FJ, Molina-Hidalgo FJ, Mercado JA, Moyano E, Rodríguez-Franco A, Caballero JL, Muñoz-Blanco J, Blanco-Portales R (2019) An atypical HLH transcriptional regulator plays a novel and important role in strawberry ripened receptacle. BMC Plant Biol 19: 586

Medina-Puche L, Molina-Hidalgo FJ, Boersma M, Schuurink RC, López-Vidriero I, Solano R, Franco-Zorrilla JM, Caballero JL, Blanco-Portales R, Muñoz-Blanco J (2015) An R2R3-MYB transcription factor regulates eugenol production in ripe strawberry fruit receptacles. Plant Physiol 168: 598–614

Merchante C, Vallarino JG, Osorio S, Aragüez I, Villarreal N, Ariza MT, Martínez GA, Medina-Escobar N, Civello MP, Fernie AR, et al. (2013) Ethylene is involved in strawberry fruit ripening in an organ-specific manner. J Exp Bot 64: 4421–4439

Migicovsky Z, Gardner KM, Money D, Sawler J, Bloom JS, Moffett P, Chao CT, Schwaninger H, Fazio G, Zhong G-Y, et al. (2016) Genome to phenome mapping in apple using historical data. Plant Genome 9: 1–15

Miron D and Schaffer AA (2005) Sucrose phosphate synthase, sucrose synthase, and invertase activities in developing fruit of Lycopersicon esculentum mill and the sucrose accumulating Lycopersicon hirsutum Humb. and Bonpl. Plant Physiol 95: 623–627

Molina-Hidalgo FJ, Franco AR, Villatoro C, Medina-Puche L, Mercado JA, Hidalgo MA, Monfort A, Caballero JL, Muñoz-Blanco J, Blanco-Portales R (2013) The strawberry (Fragaria × ananassa) fruit-specific rhamnogalacturonate lyase 1 (FaRGLyase1)

gene encodes an enzyme involved in the degradation of cell-wall middle lamellae. J Exp Bot 64: 1471–1483

Molina-Hidalgo FJ, Medina-Puche L, Cañete-Gómez C, Franco-Zorrilla JM, López-Vidriero I, Solano R, Caballero JL, Rodríguez-Franco A, Blanco-Portales R, Muñoz-Blanco J, et al. (2017) The fruit-specific transcription factor FaDOF2 regulates the production of eugenol in ripe fruit receptacles. J Exp Bot 68: 4529–4543

Moyano E, Martínez-Rivas FJ, Blanco-Portales R, Molina-Hidalgo FJ, Ric-Varas P, Matas-Arroyo AJ, Caballero JL, Muñoz-Blanco J, Rodríguez-Franco A (2018) Genome-wide analysis of the NAC transcription factor family and their expression during the development and ripening of the Fragaria × ananassa fruits. PLoS ONE 13: e0196953

Moyano-Cañete E, Bellido ML, García-Caparrós N, Medina-Puche L, Amil-Ruiz F, González-Reyes JA, Caballero JL, Muñoz-Blanco J, Blanco-Portales R (2013) FaGAST2, a strawberry ripening-related gene, acts together with FaGAST1 to determine cell size of the fruit receptacle. Plant Cell Physiol 54: 218–236

Nieuwenhuizen NJ, Chen X, Wang MY, Matich AJ, Perez RL, Allan AC, Green SA, Atkinson RG (2015) Natural variation in monoterpene synthesis in kiwifruit: transcriptional regulation of terpene synthases by NAC and ETHYLENE-INSENSITIVE3-like transcription factors. Plant Physiol 167: 1243–1258

Nitsch JP (1950) Growth and morphogenesis of the strawberry as related to auxin. Am J Bot 37: 211–215

Olsen AN, Ernst HA, Leggio LL, Skriver K (2005) NAC transcription factors: structurally distinct, functionally diverse. Trends Plant Sci 10: 79–87

Ooka H Satoh K, Doi K, Nagata T, Otomo Y, Murakami K, Matsubara K, Osato N, Kawai J, Carninci P, et al. (2003) Comprehensive analysis of NAC family genes in Oryza sativa and Arabidopsis thaliana. DNA Res 10: 239–247

Peng H, Zhao J, Neff MM (2015) ATAF2 integrates Arabidopsis brassinosteroid inactivation and seedling photomorphogenesis. Development 142: 4129–4138

Pérez-Pérez Y, Carneros E, Berenguer E, Solís M-T, Bárány I, Pintos B, Gómez-Garay A, Risueño MC, Testillano PS (2018) Pectin de-methylesterification and AGP increase promote cell wall remodeling and are required during somatic embryogenesis of Quercus suber. Front Plant Sci 9: 1915

Posé S, García-Gago JA, Santiago-Doménech N, Pliego-Alfaro F, Quesada MA, Mercado JA (2011) Strawberry fruit softening: role of cell wall disassembly and its manipulation in transgenic plants. Genes Genom Genom 5: 40–48

Quesada MA, Blanco-Portales R, Posé S, García-Gago JA, Jiménez-Bermúdez S, Muñoz-Serrano A, Caballero JL, Pliego-Alfaro F, Mercado JA, Muñoz-Blanco J (2009) Antisense downregulation of the FaPG1 gene reveals an unexpected central role for polygalacturonase in strawberry fruit softening. Plant Physiol 150: 1022–1032

Sánchez-Sevilla JF, Vallarino JG, Osorio S, Bombarely A, Posé D, Merchante C, Botella MA, Amaya I, Valpuesta V (2017) Gene expression atlas of fruit ripening and transcriptome assembly from RNA-seq data in octoploid strawberry. Sci Rep 7: 13737

Schaart JG, Salentijn EMJ, Pelgrom KTB, Aharoni A, Krens FA (2011) Isolation and characterisation of a strawberry fruit-specific promoter. Genes Genom Genom 5: 108–114

Seymour GB, Ryder CD, Cevik V, Hammond JP, Popovich A, King GJ, Vrebalov J, Giovannoni JJ, Manning K (2011) A SEPALLATA gene is involved in the development and ripening of strawberry (Fragaria × ananassa Duch.) fruit, a non-climacteric tissue. J Exp Bot 62: 1179–1188

Shan W, Kuang J-F, Chen L, Xie H, Peng H-H, Xiao Y-Y, Li X-P, Chen W-X, He Q-G, Chen J-Y, et al. (2012) Molecular characterization of banana NAC transcription factors and their interactions with ethylene signalling component EIL during fruit ripening. J Exp Bot 63: 5171–5187

Shen Q, Chen CN, Brands A, Pan SM, Ho TH (2001) The stress- and abscisic acid-induced barley gene HVA22: developmental regulation and homologues in diverse organisms. Plant Mol Biol 45: 327–340

Sugawara S, Hishiyama S, Jikumaru Y, Hanada A, Nishimura T, Koshiba T, Zhao Y, Kamiya Y, Kasahara H (2009) Biochemical analyses of indole-3-acetaldoxime-dependent auxin biosynthesis in Arabidopsis. Proc Natl Acad Sci USA 106: 5430–5435

Sun JH, Luo JJ, Tian L, Li CL, Xing Y, Shen YY (2013) New evidence for the role of ethylene in strawberry fruit ripening. J Plant Growth Regul 32: 461–470

Symons GM, Chua Y-J, Ross JJ, Quittenden LJ, Davies NW, Reid JB (2012) Hormonal changes during non-climacteric ripening in strawberry. J Exp Bot 63: 4741–4750

Tisza V, Kovács L, Balogh A, Heszky L, Kiss E (2010) Plant physiology and biochemistry. Plant Physiol Biochem 48: 822–826

Trainotti L, Pavanello A, Casadoro G (2005) Different ethylene receptors show an increased expression during the ripening of strawberries: does such an increment imply a role for ethylene in the ripening of these non-climacteric fruits? J Exp Bot 56: 2037–2046

Ulmasov T, Murfett J, Hagen G, Guilfoyle TJ (1997) Aux/IAA proteins repress expression of reporter genes containing natural and highly active synthetic auxin response elements. Plant Cell 9: 1963–1971

Usadel B, Poree F, Nagel A, Lohse M, Czedik-Eysenberg A, Stitt M (2009) A guide to using MapMan to visualize and compare Omics data in plants: a case study in the crop species, maize. Plant Cell Environ 32: 1211–1229

Vallarino JG, Merchante C, Sánchez-Sevilla JF, de Luis Balaguer MA, Pott DM, Ariza MT, Casañal A, Posé D, Vioque A, Amaya I, et al. (2019) Characterizing the involvement of FaMADS9 in the regulation of strawberry fruit receptacle development. Plant Biotechnol J 18: 929–943

Vallarino JG, de Abreu e Lima F, Soria C, Tong H, Pott DM, Willmitzer L, Fernie AR, Nikoloski Z, Osorio S (2018) Genetic diversity of strawberry germplasm using metabolomic biomarkers. Sci Rep 8: 14386

Vallarino JG, Osorio S, Bombarely A, Casañal A, Cruz-Rus E, Sánchez-Sevilla JF, Amaya I, Giavalisco P, Fernie AR, Botella MA, et al. (2015) Central role of FaGAMYB in the transition of the strawberry receptacle from development to ripening. New Phytol 208: 482–496

Villareal NM, Bustamante CA, Civello PM, Martínez GA (2010) Effect of ethylene and 1-MCP treatments on strawberry fruit ripening. J Sci Food Agric 90: 683–689

Wang Q-H, Zhao C, Zhang M, Li Y-Z, Shen Y-Y, Guo J-X (2017) Transcriptome analysis around the onset of strawberry fruit ripening uncovers an important role of oxidative phosphorylation in ripening. Sci Rep 7: 41477

Wang R, Tavano ECDR, Lammers M, Martinelli AP, Angenent GC, de Maagd RA (2019) Re-evaluation of transcription factor function in tomato fruit development and ripening with CRISPR/Cas9-mutagenesis. Sci Rep 9: 1696

Wei L, Mao W, Jia M, Xing S, Ali U, Zhao Y, Chen Y, Cao M, Dai Z, Zhang K, et al. (2018) FaMYB44.2, a transcriptional repressor, negatively regulates sucrose accumulation in strawberry receptacles through interplay with FaMYB10. J Exp Bot 69: 4805–4820

Xue C, Guan S-C, Chen J-Q, Wen C-J, Cai J-F, Chen X (2020) Genome wide identification and functional characterization of strawberry pectin methylesterases related to fruit softening. BMC Plant Biol 20: 13

Yeats TH, Migicovsky Z, Watts S, Song J, Forney CF, Burgher-MacLellan K, Somers DJ, Vrebalov J, Giovannoni JG, Rose JKC, et al. (2019) Allelic diversity of NAC18.1 is a major determinant of fruit firmness and harvest date in apple (Malus domestica). bioRxiv http://dx.doi.org/10.1101/708040

Zhang H, Kang H, Su C, Qi Y, Liu X, Pu J (2018) Genome-wide identification and expression profile analysis of the NAC transcription factor family during abiotic and biotic stress in woodland strawberry. PLoS ONE **13**: e0197892-26

Zhang S, Chen Y, Zhao L, Li C, Yu J, Li T, Yang W, Zhang S, Su H, Wang L (2020) A novel NAC transcription factor, MdNAC42, regulates anthocyanin accumulation in red-fleshed apple by interacting with MdMYB10. Tree Physiol **40**: 413–423

Zhong S, Joung JF, Zheng Y, Chen YR, Liu B, Shao Y, Xiang JZ, Fei Z, Giovannoni JJ (2011) High-throughput illumina strand-specific RNA sequencing library preparation. Cold Spring Harb Protoc **2011**: 940–949

Zhou H, Lin-Wang K, Wang H, Gu C, Dare AP, Espley RV, He H, Allan AC, Han Y (2015) Molecular genetics of blood-fleshed peach reveals activation of anthocyanin biosynthesis by NAC transcription factors. Plant J **82**: 105–121

Zhu M, Chen G, Zhou S, Tu Y, Wang Y, Dong T, Hu Z (2014) A new tomato NAC (NAM/ATAF1/2/CUC2) transcription factor, SlNAC4, functions as a positive regulator of fruit ripening and carotenoid accumulation. Plant Cell Physiol **55**: 119–135